AOWFL

Resolving Key Uncertainties of Seabird Flight and Avoidance Behaviours at Offshore Wind Farms

Annual report for April 2020 – October 2020

May 2021

AOWFL

Resolving Key Uncertainties of Seabird Flight and Avoidance Behaviours at Offshore Wind Farms

Annual report for April 2020 – October 2020

Prepared for	AOWFL
Represented by	Robin Cox, Jesper Kyed Larsen

Project Manager	Mike Armitage
Authors	Rune Skjold Tjørnløv, Henrik Skov, Mike Armitage, Mike Barker, Florence Cuttat, Katy Thomas

Project number	DHI: 11820296; RPS: ECO00516
Approval date	28 May 2021
Revision	3
Classification	Public

CONTENTS

1 Introduction

1.1 Aims and Objectives

Accurately predicting the impact of offshore wind farms (OWFs) on seabirds continues to pose a significant consenting risk for their development in the UK and Europe, due to a lack of sufficient knowledge on seabird interactions with offshore wind turbines. In turn this prevents an accurate assessment of ornithological impacts, leading to precautionary and conservative assessments which are likely to overstate the effects of OWFs on seabird populations.

The aims of this Project are to collect evidence on seabird flight patterns and behavioural responses to offshore wind turbines, with the ultimate objective of informing and refining predictive models for collision risk assessments.

The focus is on seabird flight behaviour during the breeding period and post-breeding period, i.e. during the period when seabirds are commuting from their breeding colonies to their offshore feeding areas, and in particular for the target species: northern gannet (hereafter 'gannet'), black-legged kittiwake (hereafter 'kittiwake') and large gulls (herring gull, lesser black-backed gull and great black-backed gull).

The main objectives were to collect species-specific data on three-dimensional (3-D) flight behaviour to document:

- Micro-avoidance behaviour – flight behaviour within and in the immediate vicinity of individual wind turbine rotor swept areas, including flight speeds and flight heights, and collision events; and

- Meso-avoidance behaviour – flight behaviour within and in the immediate vicinity of the wind farm, including flight speeds and flight heights.

This annual report evaluates the data collected during the 2020 breeding season.

1.2 Report Structure

This report evaluates the data collected between the 1st April and 31st October2020, summarising the main findings relating to the objectives above:

Section 1 includes a brief introduction and background to the study;

Section 2 provides a list of definitions which have been used throughout the report;

Section 3 details the equipment and systems implemented as part of the study and its deployment offshore. An overview is also provided on the methods applied for video analyses;

Section 4 presents statistics on collected data;

Section 5 presents seabird temporal dynamics analysed from video recordings;

Section 6 presents meso-avoidance analyses of changes in track density and flight direction of target species in relation to distance (100 m +) to turbines and wind speed;

Section 7 presents micro-avoidance analyses and observed flight behaviour in the vicinity of the rotor swept zone;

Section 8 provides analyses of changes in flight height of target species in relation to distance (100 m +) to turbines and bird behaviour;

Section 9 provides analyses of flight speeds of target species in relation to distance (100 m +) to turbines and bird behaviour.

Section 10 provides analyses of flight directions of target species in relation to distance (100 m +) from the rotors and rotor orientation.

Section 11 discusses the main findings of the study (to date) and recommendations for further improvement to sensor equipment and design and the analytical framework.

1.3   Study Area and Project Design

The study site is the European Offshore Wind Deployment Centre (EOWDC), situated 3 - 4.9 km off the coast of Aberdeen in north-eastern Scotland. The site was considered suitable for the study based on its location close to breeding colonies and offshore feeding grounds of gannet, kittiwake and large gulls and previous surveys in the area.

In order to fulfil the Project aims and objectives, an integrated radar-camera monitoring unit was deployed on the EOWDC which was capable of generating 3-D flight tracks, supported by video footage. This enabled identification of birds as they moved through the wind farm. This is discussed further in Section 3.

The Project is focussed on diurnal flight activity during the breeding season (as described in Section 1.1) and post-breeding dispersal (i.e. April - October) in 2020 and 2021. The time schedule for the Project activities is provided in the Project Implementation Plan (PIP) (DHI *et al.,* latest iteration in July 2020).

1.4   The Project Implementation Plan (PIP)

The PIP is a live document which continues to be updated throughout the Project and includes details on the hardware and software design, field tests, factory tests and the analytical and reporting framework applied for monitoring flight patterns and avoidance responses of the target species within the EOWDC using the MUSE system.

The Project takes into account several lessons learnt from the ORJIP Project[1] (Skov *et al*., 2018), further details of which can be found in the PIP.

---

[1] The ORJIP (Offshore Renewables Joint Industry Programme) Bird Collision Avoidance (BCA) Study was carried out between 2014 – 2017 at Thanet Offshore Wind Farm. The study aimed to develop a bird monitoring system to detect and track bird movements around the wind farm by deployment of a multi-sensor monitoring system with the objective of quantifying empirical avoidance behaviour

2 Definitions

Table 2.1 provides a glossary of terms and definitions which are used throughout this report.

Table 2.1: Glossary of terms

Term	Definition
AOWFL	Aberdeen Offshore Wind Farm Limited
Avoidance behaviour	Any action taken by a bird, when close to an operational wind farm, which prevents collision (SNH, 2010). Such action may be taken early enough to avoid entering into the wind farm (macro-avoidance) or taken within the wind farm, avoiding the rotor swept zone (RSZ) (meso-avoidance) or individual turbine rotor blades (micro-avoidance)
Avoidance rate	Correction factor applied in collision risk models in order to take account of the likely degree of successful avoidance of a bird colliding with the turbine rotors
AWF06 and AWF10	Turbines 6 and 10 within the EOWDC wind farm
Collision risk	Risk of injury or death caused by an encounter or collision with turbines or rotor blades at a wind farm (Band, 2012)
Clutter	Clutter is a term used for unwanted echoes in electronic systems, particularly in reference to radars. Sea clutter refers to those echoes returned from the sea surface, which can cause serious performance issues with radar systems
Detection probability	Probability for the sensor to pick up a bird or a flock of birds, which is dependent on distance, orientation, shape, size, clutter, etc. The maximum detection is the distance where the detection probability falls below 0.5 (equal chance of detecting a bird or not)
EOWDC	European Offshore Wind Deployment Centre
Meso-avoidance	Bird behavioural response within the wind farm footprint to individual turbines (considering a 10 m buffer around the rotor swept zone (RSZ)) and resulting in a redistribution of the birds within the wind farm footprint
Micro-avoidance	Bird behavioural response within 10 m of the rotor swept zone, considered as the bird's 'last-second action' taken to avoid collision with a rotor blade
MUSE	Multi-sensor high-speed processing software which facilitates the communication between radar and camera equipment
Rotor	Part of a wind turbine that extracts kinetic energy from the air and coverts this wind into rotational energy in the drive train. The current generation of horizontal axis turbines have rotors with three blades. In the context of this analysis the 'rotor' also defines the ellipse representing the blades at a given time.
Rotor swept zone (RSZ)	Zone swept by the rotating turbine blades (the rotor) of a wind turbine. For the purposes of analysing empirical micro-avoidance, the RSZ refers to the circle drawn by the rotor blades. As viewed from above, while the rotor refers to the ellipse representing the blades at any given time

Term	Definition
Sensor	The radars and cameras used in this study to detect flying seabirds and collect bird behavioural information at different scales (meso-, micro-) as well as data on flight heights
Track	Recorded trajectory of one or a group of several birds by the study sensors. A track is made of different recorded positions or nodes
Track density	Estimation of empirical avoidance rates based on a ratio of the density of bird tracks detected in avoidance/non-avoidance areas. This can be estimated using the number of tracks within a given area, or using the lengths of tracks within a given area

3 MUSE System

The following section provides an overview of the sensor and software settings and of the methods employed during video analyses. Full details of the technical and functional specifications of the hardware and information on sources of uncertainty in the analytical framework can be found in the PIP (DHI *et al.*, 2020).

3.1 Overview of sensors and software settings

The radar-camera monitoring unit deployed on the EOWDC collects radar tracks and video footage enabling species identification and analysis of meso- and micro-avoidance behaviours in an operational OWF. The communication between the camera and radar is facilitated by a multi-sensor, high-speed processing software (DHI MUSE); this software allows birds discovered by the radar to be automatically targeted by the cameras and followed, using motion detection and video.

The radar (Furuno FAR-3000) is oriented horizontally and movements of birds in the wind farm area are tracked automatically. Tracking information from the radar is continuously recorded to a geo-database by the system. For the sample of radar tracks that have triggered video recording, they are combined with images from the camera which are flagged with the same track identification. Information about the height of the bird is also recorded during the period it is viewed by the camera; the target's height is calculated using the MUSE software by triangulation of the combined distance measurements from the radar and the measurements of inclination angle by the camera. Full details of the technical and functional specifications of the radar are provided in Table 3 of the PIP.

In this project, the camera setup consists of two pan-tilt cameras. One camera is a FLIR M400 combined long-range zoom daylight camera and thermal sensor to allow recordings of seabird behaviour also during darkness. The other, a RVision MiniHP, is a rugged daylight camera comprising a pan-tilt housing; the range at which movements of seabirds can be tracked by motion detection is approximately 1000 m, and the minimum distance is approximately 50 m. Full details of the technical and functional specifications of the radar are provided in Table 4 of the PIP.

The radar and the FLIR M400 camera are installed on AWF10, while the RVision MiniHP is installed on AWF06. The detection and tracking ranges of the radar and cameras are illustrated on Figure 1 below.
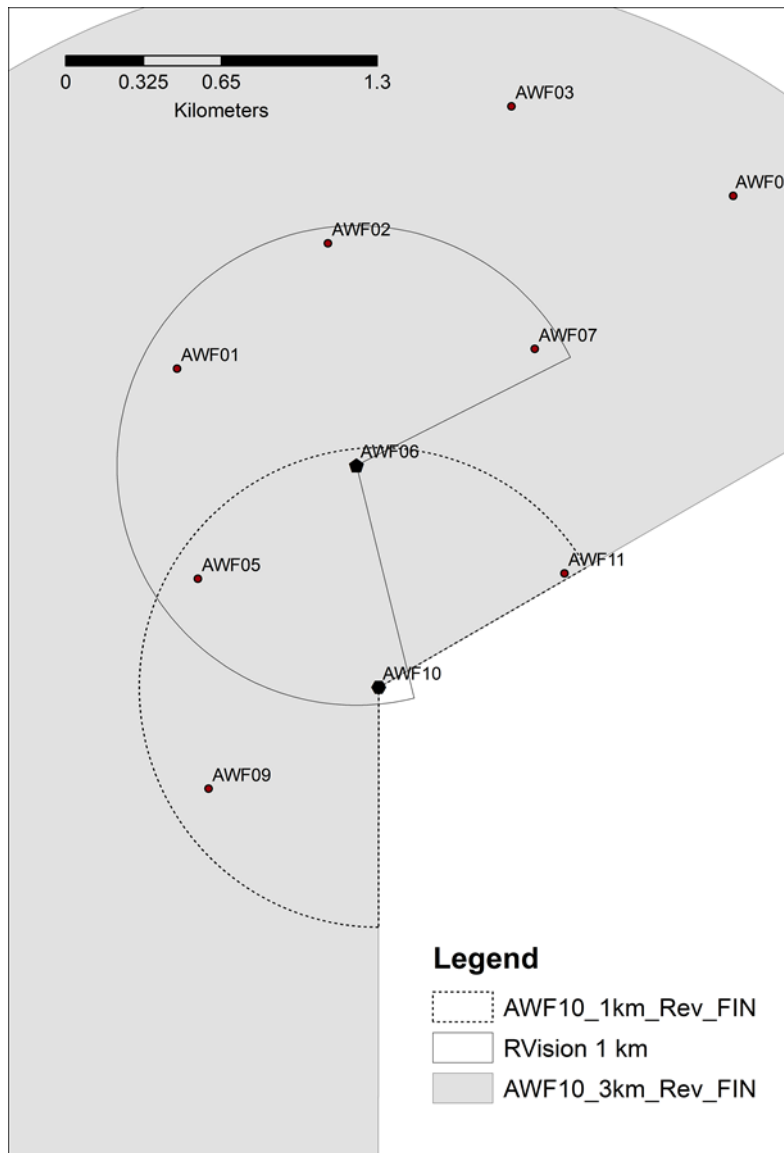
Figure 1 Set up and tracking ranges of the EOWDC radar and cameras

Prior to installation, field tests were undertaken at a coastal test location in Ebeltoft, Denmark, which are detailed within Section 3.2.3 of the PIP (DHI *et al*., 2020).

Checks and calibration of all radar signal processing in the MUSE software were carried out in a laboratory. The database storage was tested with track data from the field; the MUSE system saves all bird tracks as geo-referenced tracks with unique ID which includes a timestamp. Parameters included and checked in the database include UTM coordinates for each node in the tracks, order of track nodes, flight direction, variation of flight direction and flight speed. The alignment of the camera with the initial target position was tested by including annotations of the angle, elevation and zoom level in the video output from the camera.

Following calibration of the radar, the cameras were calibrated remotely to optimise focus and zoom levels, motion detection controls and division of the scanned area between cameras.

In addition to empirical tests of the detection probability of the FAR-3000 radar carried out in 2016 (DHI 2017) a series of theoretical (modelled) tests of the vertical coverage and detection probability of different sizes of birds (radar cross sections) were made on the computer. The results showed

good detection of passerines to 3 km, of gulls to 4 km, of gannets to 5 km and of large flocks of birds to 6 km during calm sea states, with detection probability dropping at higher sea states (4+).

Full details of the field and factory tests and configuration undertaken on the camera and radar equipment are provided in Sections 3.2 - 3.4 of the PIP.

3.1.1 Operating modes

Data on meso- and micro-avoidance of seabirds can be collected in two different sensor modes; dual mode and solo mode.

Sensor dual mode with integrated radar and camera tracking was the priority mode of operation during the 2020 breeding season as it allowed for 3-D tracks and estimation of flight heights through triangulation of the radar (distance) and camera (inclination angle) for any given track. In this mode the radar will always trigger the camera to record the bird movement by motion detection, and unless the camera is engaged in tracking it is available to receive information on bird targets from the radar.

The camera records the bird movement for as long as the bird can be detected by the camera's motion detection. If the camera loses the target, information on the location of the bird is transferred from the radar to the camera, in which case it is able to continue following the bird.

The performance of the radar is affected during strong weather conditions in which high waves cause the dynamic clutter filter in the MUSE software to generate a high level of false negative bird detections (failure to record birds), which affects the system when operating in dual mode. During such conditions, it is possible for the system to operate in solo mode, when the camera is moved to a fixed position and awaits a target to follow by motion detection. In solo mode, a bird's movement will be followed and recorded if a bird is detected in the camera frame; however, no associated radar track of its position is generated. The use of solo mode has the potential to increase the sample size of videos of birds' movements but is subject to a higher degree of subjectivity in the analysis of the birds' flight behaviour and position in space.

During the 2020 breeding season, the system was only operated in dual mode with camera recordings being triggered only by radar to optimise the number of coupled radar-camera tracks collected and thereby enhancing the assessment of 3-D avoidance behaviour.

3.2 Overview of methods applied for analyses of flight behaviour

3.2.1 Meso-avoidance behaviour

The meso-avoidance behaviour was assessed for the target species: gannet, lesser black-backed gull, herring gull, great black-backed gull and kittiwake. Species and species groups were identified using video data. Although only a proportion of all radar tracks were associated with videos, the videos are considered to be representative for the composition of bird species recorded by the radar. This is especially the case during the 2020 breeding season when the cameras were only recording when triggered by the radar. The videos with information on birds were extracted automatically from the total sample of all videos (which includes videos containing no birds) by using an AI-based screening algorithm. The classification of flight behaviour by the video analysts was based on a subjective judgement of the bird's movement in the video recording in relation to feeding/commuting flight patterns and relative to the location of the turbines seen in the video. A second pass of the videos was also undertaken by a second experienced analyst and any discrepancies were highlighted for review and agreement.

The meso-avoidance behaviour was quantified based on distributional patterns which are assumed to be the result of avoidance behaviour at these scales. Species-specific meso-avoidance

behaviour was analysed 3-dimensionally by using gradients in the following derived flight parameters which combined radar tracks and dual-mode videos:

- Mean track length density;
- Mean flight height;
- Mean flight speed; and
- Mean change in flight direction relative to the orientation of the rotor.

The flight statistics of the above parameters were calculated separately for feeding and commuting individuals as judged from the videos.

3.2.2 Micro-avoidance behaviour

Micro-avoidance behaviour was primarily quantified by calculating the proportion of birds adjusting/not adjusting to the presence of the rotors. The video data was screened to ensure quality data for the micro-avoidance analysis using the same process as applied in the ORJIP BCA project[1]. The screening process consisted of three subsequent steps which included removing irrelevant material of movements other than birds, low quality video material and re-assessing previously coded behaviour. A quality assurance process was used to provide second opinion on species identification for all gull species.

The micro-avoidance analysis considered the behavioural reaction of the bird(s) to the orientation of the rotor and the presence of blades when entering the rotor swept zone (RSZ) and a 10 m buffer around it, unlike the meso-avoidance analysis, where only the position of the collected data was considered. The micro-avoidance behaviours were coded into one of the following five categories:

- Adjusting by returning before crossing the RSZ;
- Adjusting by stopping before crossing the RSZ;
- Adjusting flight path relative to rotor orientation when crossing the RSZ, sub-divided into different types of paths, i.e. perpendicular, oblique, along, etc;
- Non-adjusting flight path and crossing the RSZ; or
- Collision.

Figure 2 below illustrates the assessment scheme for micro-avoidance behaviour within the RSZ; within the RSZ (blue circle) and 10 m buffer (red circle) black arrows represent bird movement in relation to the rotor (dark blue ellipse + 10 m). The light blue arrow represents the wind direction.
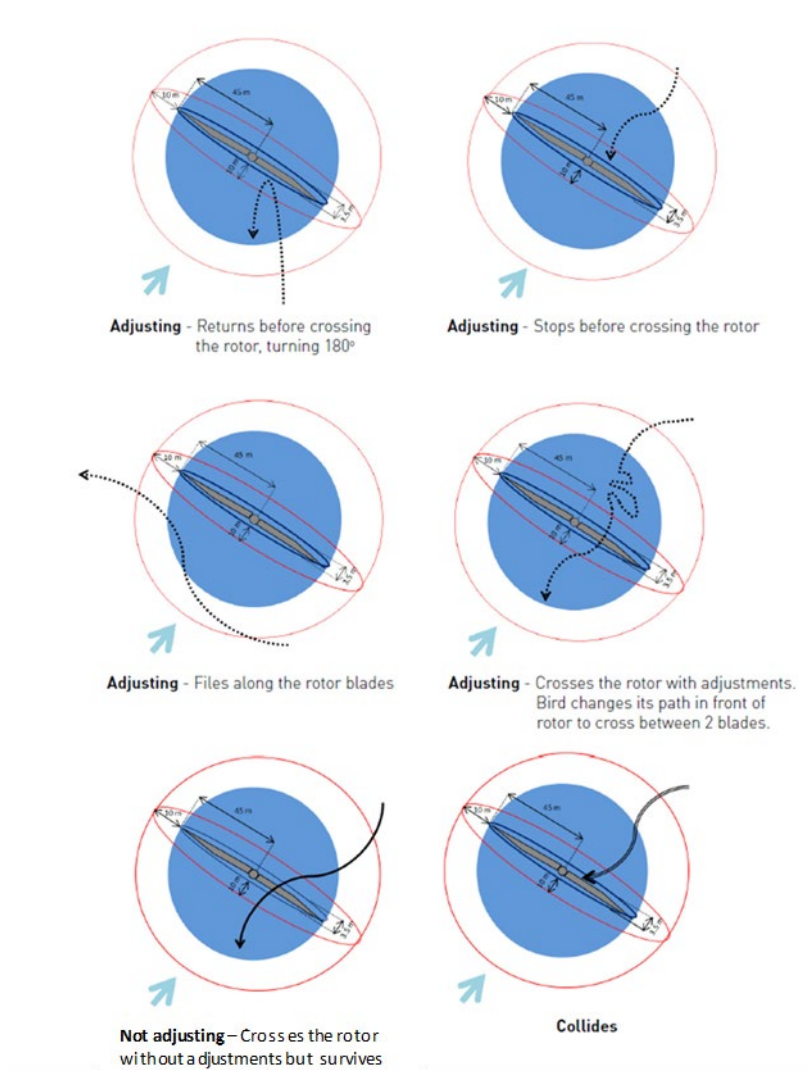
Figure 2 Assessment scheme for micro-avoidance behaviour (source: altered from the ORJIP project)

The analytical frameworks associated with the two modes of sensor operation are shown in Figure 3.
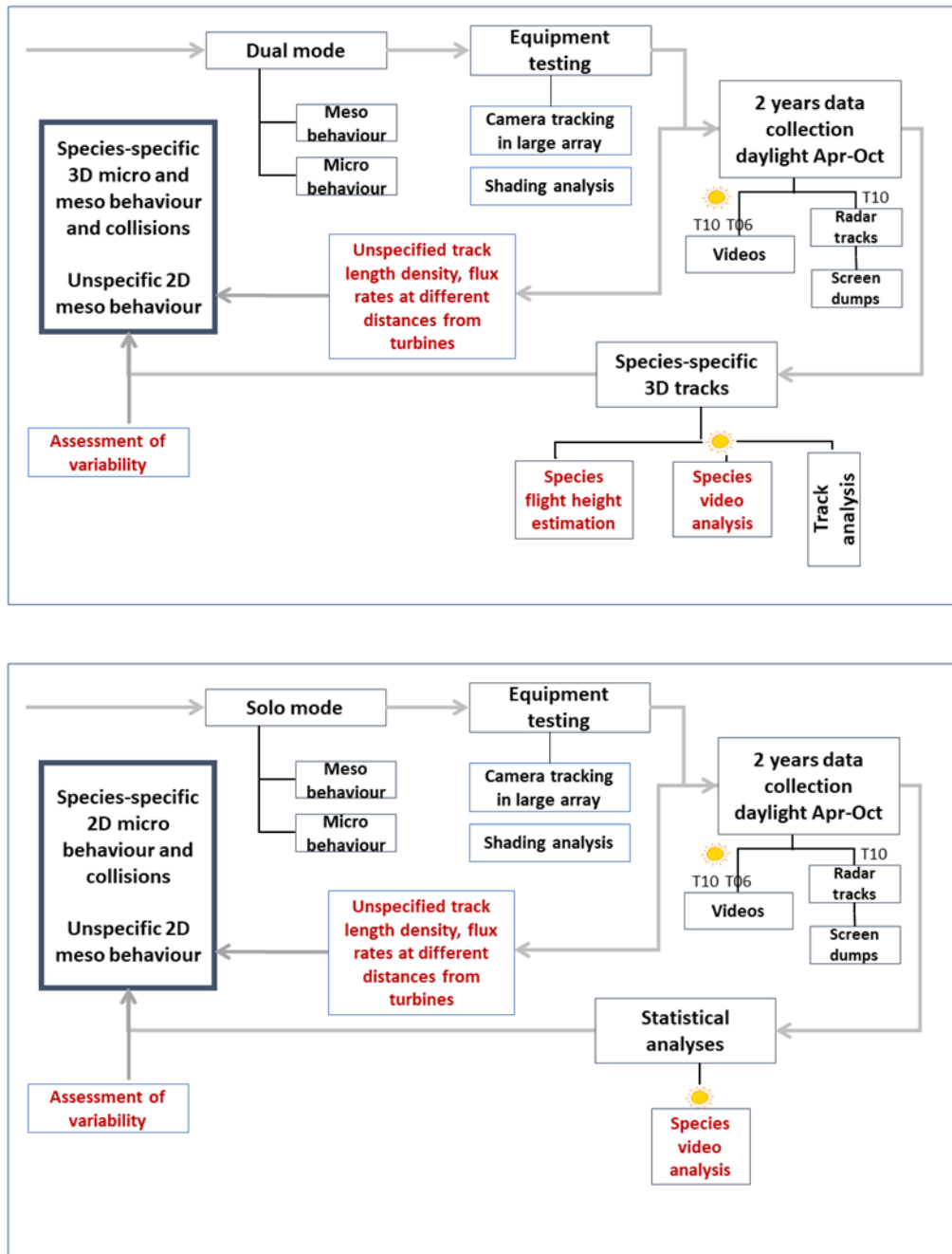

Figure 3 Overview of the analytical framework of the EOWDC Project

3.2.3 Collisions

No collisions have been recorded in the videos in the 2020 survey period. If any are recorded in future, they will be analysed in order to provide documentation of movement patterns and flight behaviour associated with each collision event; species will be determined to the highest possible taxonomic level. If possible, the collision event will also be stratified by the location of the turbine and the weather conditions.

3.2.4 Flight altitude, flight speed and flight direction

Flight height was estimated by triangulating the radar and video recordings of the same individual in close to real time for selected species. The estimated flight height was added to the video track data. The resolution of the 3-D tracks was similar to the 2-D tracks (approximately 30 m between track nodes) which was sufficient to generate good statistics on flight heights.

Seabird flight speeds in the wind farm were estimated from the radar tracks as the mean speed per segment of a track rather than the mean speed measured over the whole track.

Flight directions were assessed from the radar tracks by calculating the direction of a bird relative to the orientation of the rotors at that time. The orientation of the rotor was taken as perpendicular to the wind direction measured in the wind farm by Vattenfall at hourly intervals.

3.2.5 Assumptions and limitations

The MUSE software processing the signals from the FAR-3000 radar operates a series of clutter filters with the main function to eliminate noise (clutter) before saving the data to tracks. In an offshore environment, dynamic noise filters are essential for reducing the effect of noise induced by waves and precipitation. The filtering of wave clutter is the most important, and it works by adapting its filtering level dynamically in response to the intensity of waves. The result of the dynamic clutter filter is that when signals from noise increase in volume and Db-value due to rising sea state the clutter elimination will erase an increasing proportion of bird echoes. The effect of the dynamic clutter filter translates into significant false negative bird detection rates during adverse conditions. Another effect of the dynamic clutter filter is a low level of false positives in all conditions.

As a consequence, using the radar data to quantify traffic rates of birds through the wind farm is therefore only possible by application of correction factors for the different wind speeds/sea states which will require a considerable collection of additional data on false negative radar recordings. Similarly, the cameras can only track one target at a time and therefore do not collect data on accurate passage rates of birds through the wind farm. Using the radar data to control the cameras is also limited by the effect of rising sea states on false negative recordings. The radar may still record birds during adverse conditions, however applying the solo mode for the cameras during such conditions may result in more video documentation of seabird behaviour being collected during high sea states. The analytical framework used in the study has fully accounted for these limitations by applying statistics on the collected parameters of seabird flight behaviour which are insensitive to false negative recordings by the radar during the higher sea states.

Both the radar and camera data have high spatial resolution and no doubt contain a relatively high level of autocorrelation. This annual report only presents the data as collected without attempting to control for the autocorrelation. Thus, the significance of the flight and avoidance patterns remains to be formally tested. The patterns will be analysed in the final report using mixed regression models which incorporate an autocorrelation structure to enable unbiased assessments of the effect of distance to rotor and weather conditions on flight parameters.

The meso avoidance analyses assume that the track density (track length per unit area) in the absence of the wind farm would have been uniform inside the wind farm, i.e. one would have observed the same track density both inside and outside the non-avoidance zone near the rotor within the wind farm area (in the absence of the wind farm). The baseline data on the densities of target species in the EOWDC have not yet been checked in order to confirm whether this is a realistic assumption. Species identification may not be possible for all targets detected by the system, as it depends on visibility conditions and proximity of targets. In addition, although a large range of weather conditions have been captured in data collected, the data used in the quantification of meso and micro avoidance is limited to daytime, and therefore there is associated uncertainty on whether the data represents poor visibility and night conditions. The cameras can only track one target at a time and therefore do not collect data on accurate passage rates of birds through the RSZ. Accordingly, they do not provide absolute number of collisions.
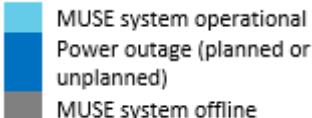
4 Equipment Performance Statistics

4.1.1 Performance

The system has collected a large sample of radar tracks and videos during the April to October 2020 period. Many of the videos contained more than six camera movements, indicative of the system following a bird movement. The number of estimated height measurements was very high, and a good proportion (>30%) of the collected videos reflected tracks with more than nine flight height estimates. The daily totals reflected a large variation in bird flight activity and the temporal differences are discussed in Section 5. Details of the sample sizes are in section 4.1.2.

There were a number of technical and other issues that affected the operation of the system and causing it to be offline for some periods. These are shown in Table 4.1 and highlight that the system was operational for 57% of the target season. The outage issues can be classified as (1) SIM capacity (early April); (2) planned power outages in May and June and an unplanned power outage in June; (3) reboot malfunction following power outages due to flat BIOS battery requiring a manual reboot which was hindered due to Covid restrictions on the site team's capacity to access the system; and (4) radar-camera communication being offline.

Table 4.1: Planned and unplanned outages in 2020

A summary of the performance indicators of the radar and camera equipment deployed on AWF06 and AWF10 is shown in Table 4.2. There is an improving pattern showing system coverage for both the radar and the cameras strengthening through the season to greater than 95% by the end of the season. This high coverage is expected to be carried forward into the 2021 season of data collection.

Table 4.2: Performance indicators of radar equipment and cameras on AWF06 and AWF10

Month	Radar track data coverage (%)	Camera AWF06 coverage (%)	Camera AWF10 coverage (%)	Radar screen images (%)
April 2020	27	10	10	27
May 2020	26	26	26	26
June 2020	33	33	33	47
July 2020	61	52	52	77
August 2020	87	87	87	90
September 2020	94	78	94	81
October 2020	98	97	97	98
Average	61	55	57	64

4.1.2 Sample Sizes

A summary of the number of radar tracks and videos is shown in Table 4.3 and illustrated on Figure 4 below. The video level is a measure of the number of times the camera moves when tracking a target by motion detection, where the higher the level, the more likely it is that the video is recording the movement of a bird.

Table 4.3: Sample sizes of radar tracks and videos with associated video levels

Month	Number of radar tracks	Number of videos				
		Level 0*	Level 1-2*	Level 3-5*	>= Level 6*	Total Number
April 2020	68,367	342	51	37	40	470
May 2020	147,990	2,420	618	333	359	3,730
June 2020	88,638	7,418	1,273	358	285	9,334
July 2020	72,169	3,920	844	393	313	5,470
August 2020	183,904	10,666	2,658	782	876	14,982
September 2020	184,486	9,085	1,695	1,410	1,290	13,480
October 2020	213,477	6,265	1,647	953	866	9,731
Average	137,004	5,731	1,255	609	576	8,171
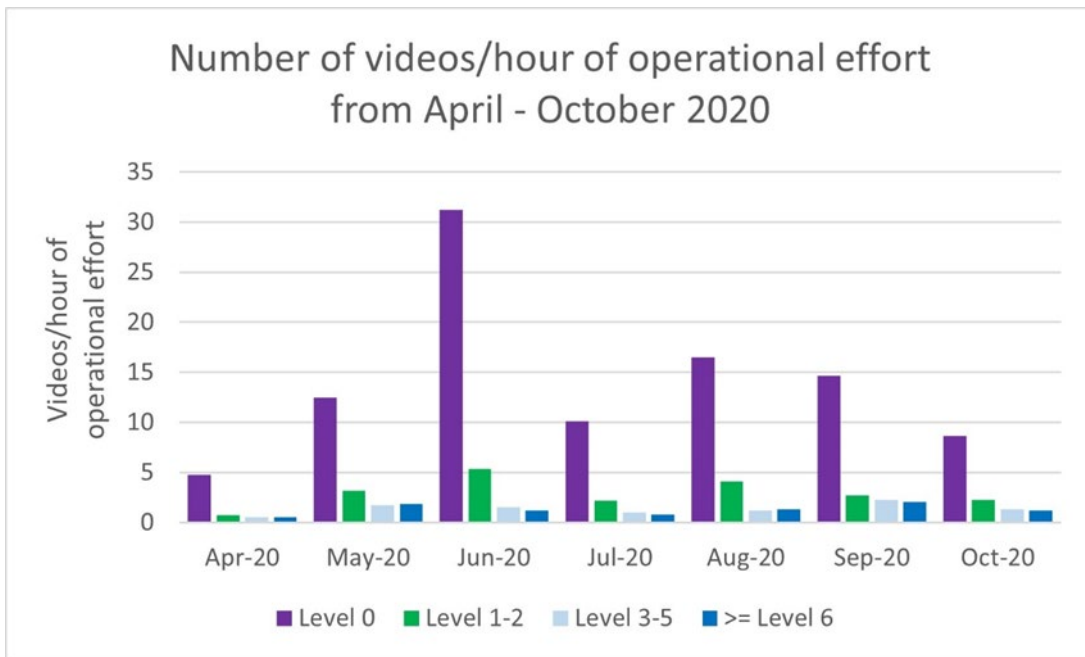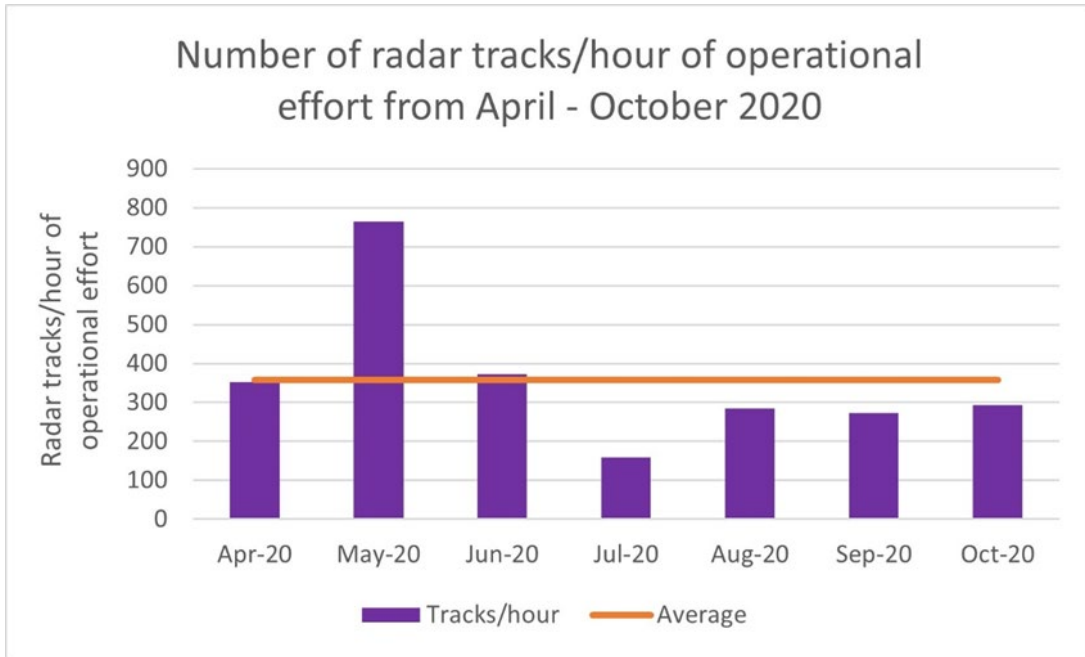
Figure 4 Statistics showing monthly collection of radar and video data per hour of operational effort (total combined day and night videos)

5   Seabird temporal dynamics

The video data collected from cameras on turbine 6 and 10 showed a considerable temporal variation in bird activity over the analysed period from April to October 2020. The videos revealed relatively low levels of bird activity during spring continuing until mid-summer (April – July) followed by a prolonged period with much higher activity in late summer and autumn (August – October). April and May had relatively low levels of bird activity with small numbers of large and small gulls, gannets, terns and few procellarians (fulmars, shearwaters and storm petrels) and skuas recorded (Fig. 5 – 8). Both June and July were rather quiet with small numbers of unidentified large gulls and herring gulls and in July a few procellarians were recorded (Fig. 5 and 8). In August, the level of activity increased considerably with large numbers of unidentified large gulls and herring gulls. Moreover, kittiwakes, gannets, auks, procellarians and skuas were all recorded in small numbers. Over the studied period, September was the peak month for the most commonly recorded species at the wind farm. Recorded numbers of both unidentified large gulls, herring gulls, kittiwakes and gannets increased to more than 1,000 birds in September. September was also the peak month for terns with large feeding flocks recorded. Procellarians and skuas also peaked in September but were scarcer (Fig. 8). Despite a continued high diversity of species, bird activity in October reduced to a similar level as recorded in August. Mixed feeding aggregations of auks, kittiwakes and herring gulls were frequently recorded in the wind farm during the period between mid-August and early October.
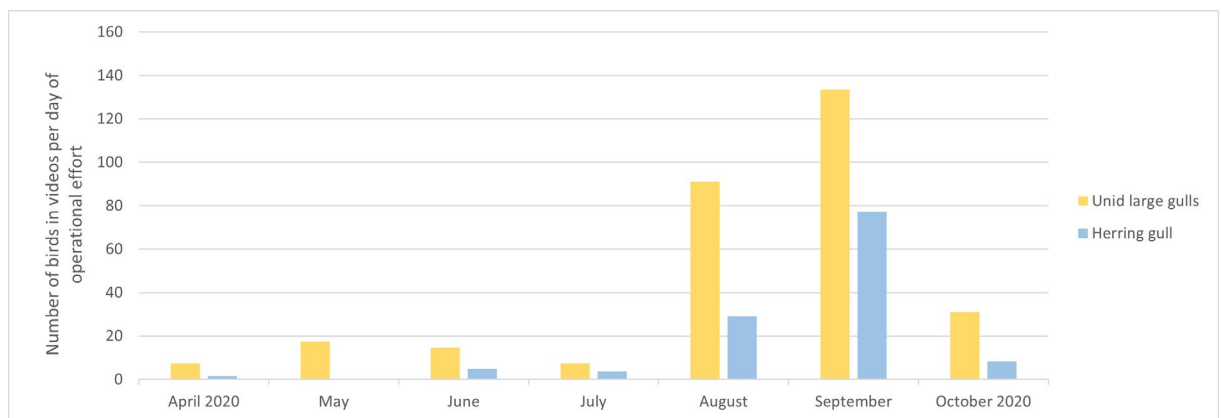

Figure 5 Number of unidentified large gulls and herring gulls in bird videos per day of operational effort from April – October 2020.
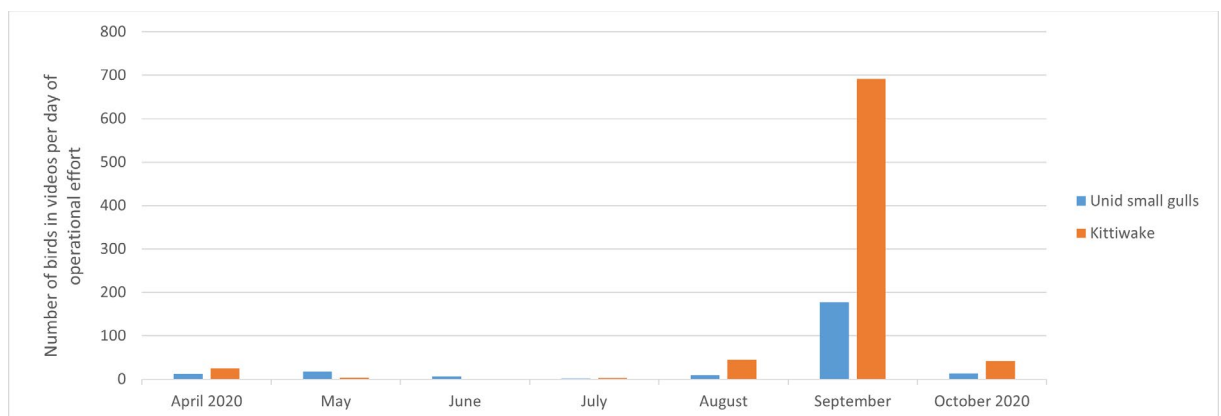

Figure 6 Number of unidentified small gulls and kittiwakes in bird videos per day of operational effort from April – October 2020.
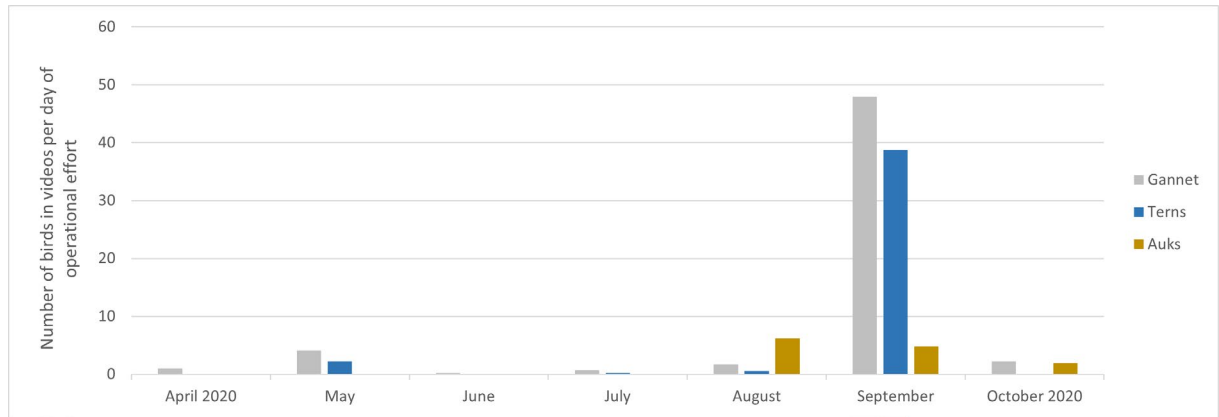
Figure 7 Number of gannets, terns and auks in bird videos per day of operational effort from April – October 2020.
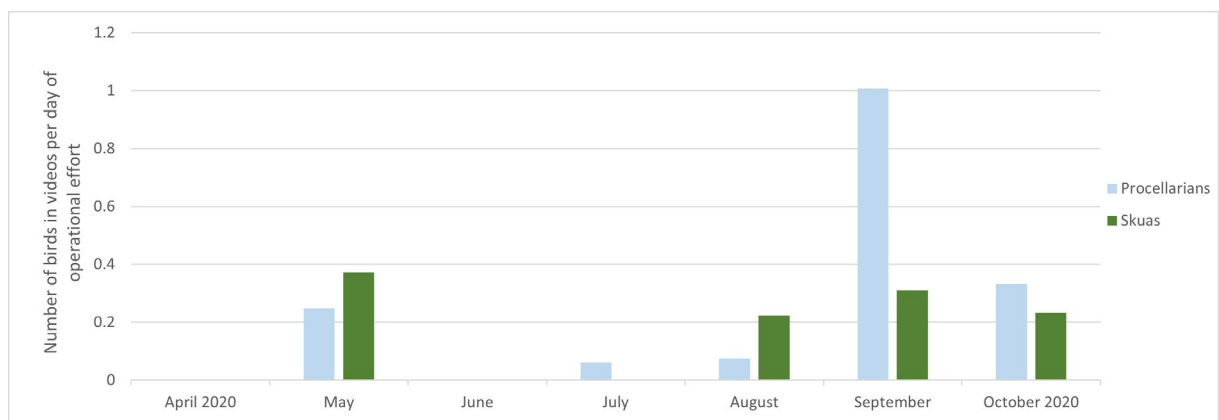

Figure 8 Number of procellarians (shearwaters, storm petrels and fulmars) and skuas in bird videos per day of operational effort from April – October 2020.

Disregarding the potential difference in the ability of the radar to locate and track differently sized birds at high wind speeds and sea states we analysed the frequencies at which target species appeared in the videos in relation to wind speed. The dynamic clutter filters used in radar software is known to influence false negative detection rates during high sea states (see section 3.2.5).

The frequency of different bird species recorded during autumn 2020, where bird activity was high, varied with the prevailing speed of the wind. Because some wind speeds may dominate for longer periods of time or be generally more regular than other wind speeds, we accounted for this potential bias in time by computing the number of some of the most commonly recorded species or species groups per hour of wind speed in three classes: <5 m/s, 5-8 m/s and >8 m/s (Fig. 9 – 11). During August – October 2020 the operational performance of the cameras was high (> 86%) and comparable between months, and hence, correction of bird numbers to account for operational performance during the three classes of wind speed was considered unnecessary. Consistently through August – October, unidentified large gulls and herring gulls were mainly recorded in light winds below 8 m/s. In fact, the majority of large gulls were recorded at low wind speeds <5 m/s (Fig. 9). During the peak period in September, small gulls and kittiwakes were mainly recorded in medium wind speeds between 5-8 m/s and in strong winds >8 m/s (Fig. 10). In contrast to the gulls, the vast majority of gannets were recorded in strong winds (Fig. 11).
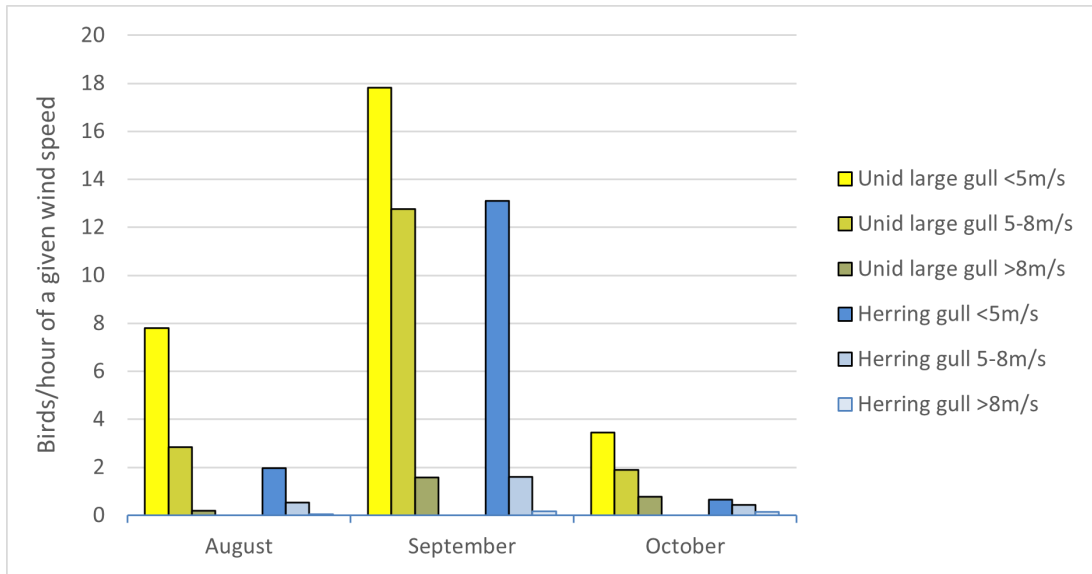
Figure 9 Number of unidentified large gulls and herring gulls recorded per hour of wind speed (<5m/s, 5-8m/s, >8m/s) during the months of high bird activity from August – October 2020.
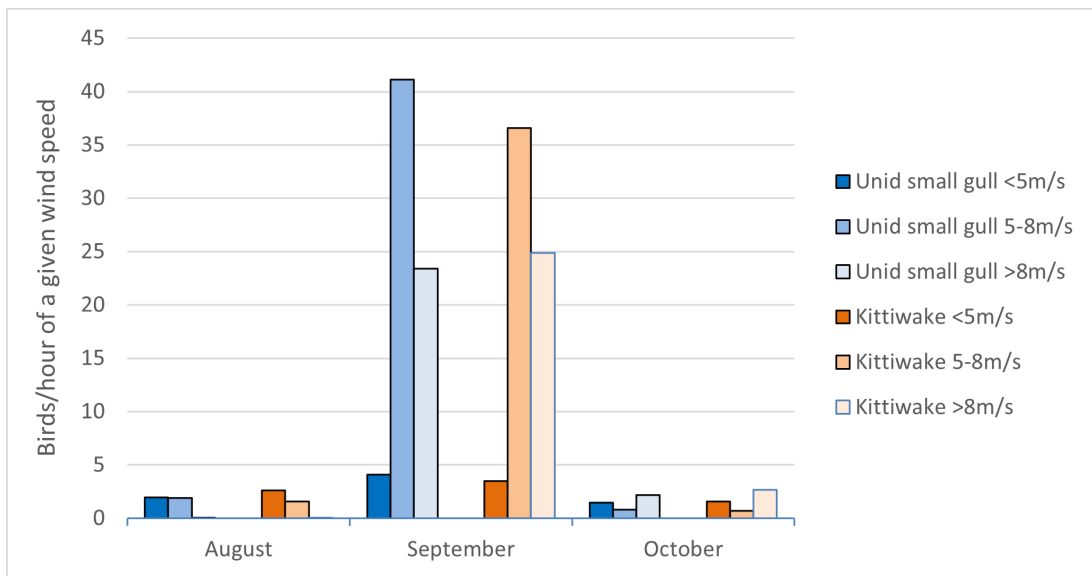

Figure 10 Number of unidentified small gulls and kittiwakes recorded per hour of wind speed (<5m/s, 5-8m/s, >8m/s) during the months of high bird activity from August – October 2020.
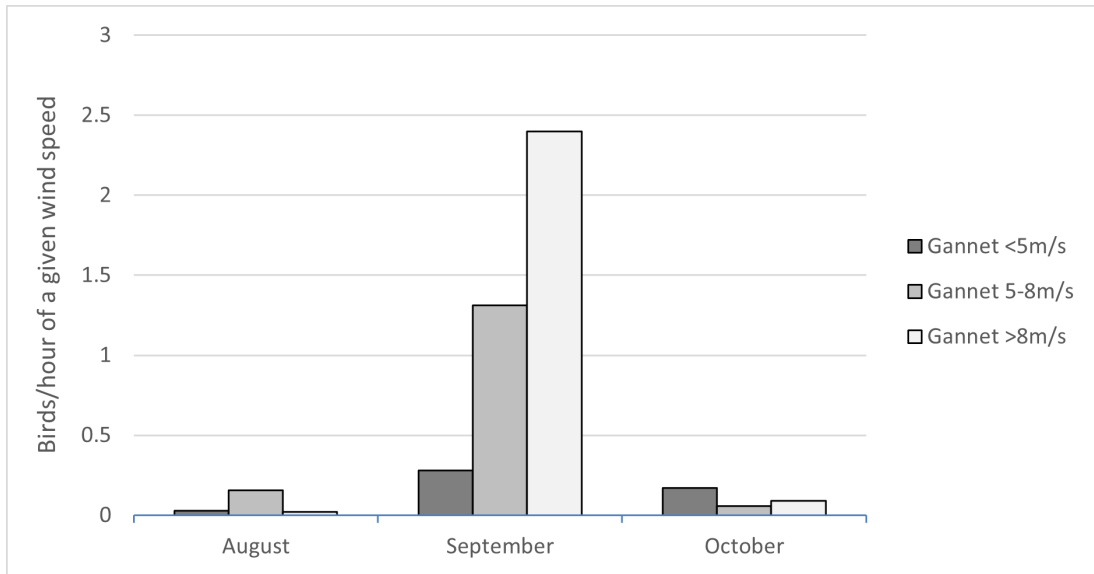
Figure 11 Number of gannets recorded per hour of wind speed (<5m/s, 5-8m/s, >8m/s) during the months of high bird activity from August – October 2020.

As a result of the temporal pattern of occurrence and absolute numbers recorded, the monthly composition of species changed noticeably over the study period from April – October 2020. In April, diversity was low with gulls, kittiwakes and gannets as the predominant species or species groups (Figure 12). Diversity increased in May with great black-backed gulls and skuas recorded in a small proportion of the videos along with a much larger proportion of gulls, terns, kittiwakes and gannets (Figure 13). Unidentified large gulls and herring gulls constituted the largest proportions of birds recorded by the cameras in June (Figure 14). July was roughly similar to June in species composition but had a larger proportion of videos with kittiwakes (Figure 15). August had a higher diversity compared to previous months with lesser and great black-backed gulls, auks, terns, skuas and cormorants recorded in small proportions (Figure 16). In September, the high diversity continued but kittiwakes were recorded in a larger proportion of the videos compared to the previous month (Figure 17). The species composition in October was similar to the species composition recorded for August and a continued high diversity of species (Figure 18).
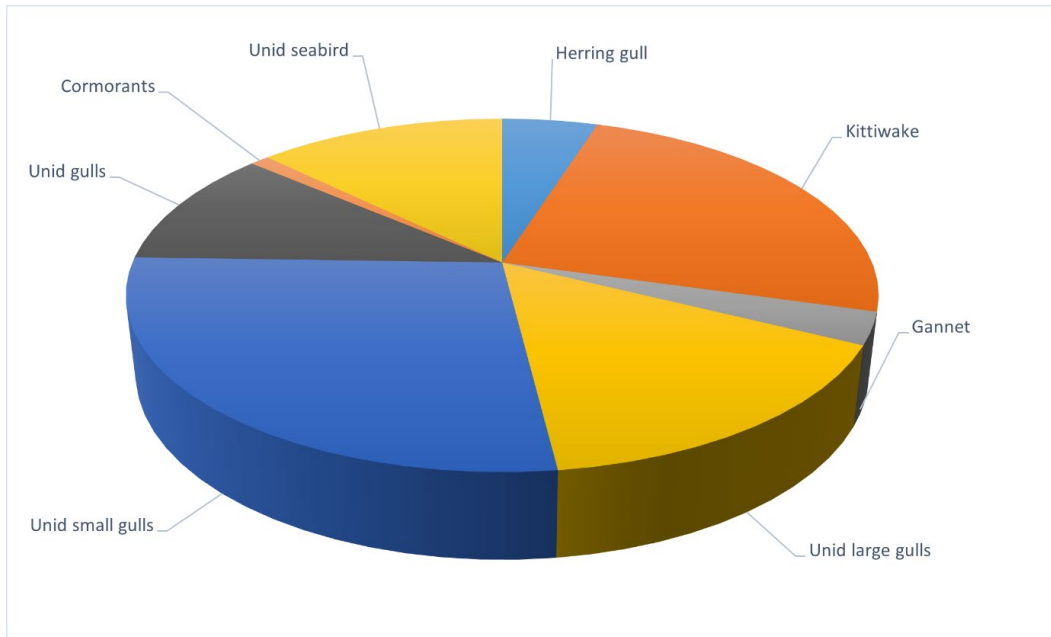
Figure 12 Proportions of species and species groups in April 2020.
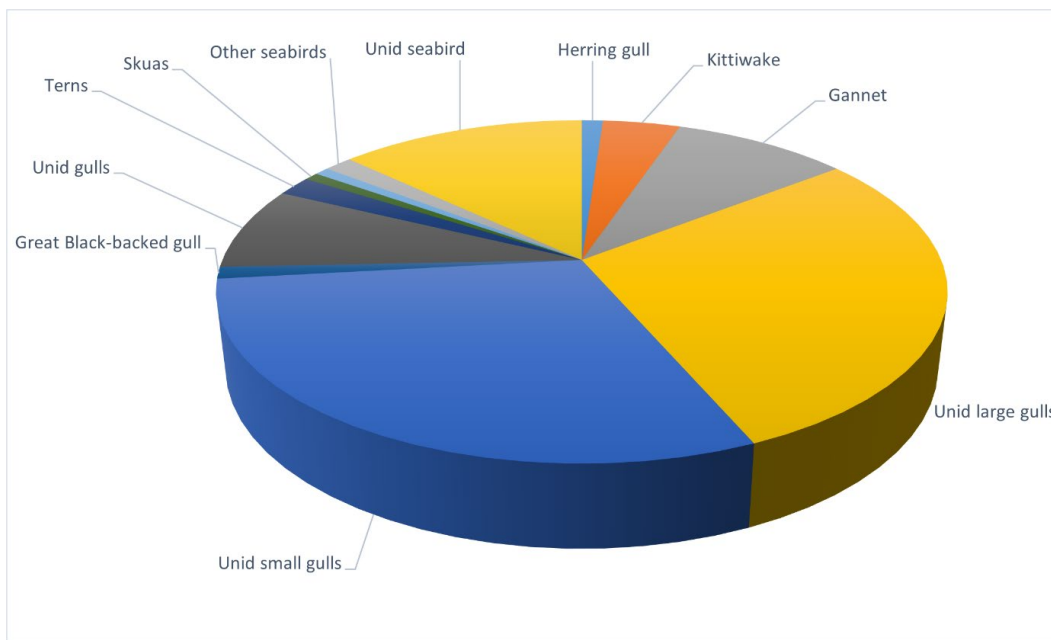

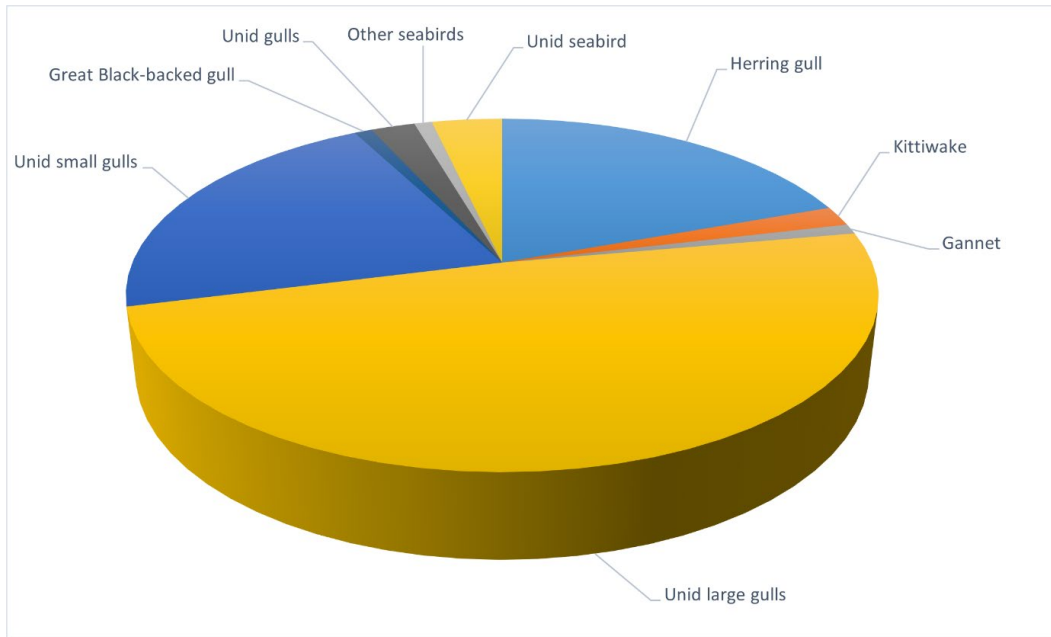Figure 13 Proportions of species and species groups in May 2020.

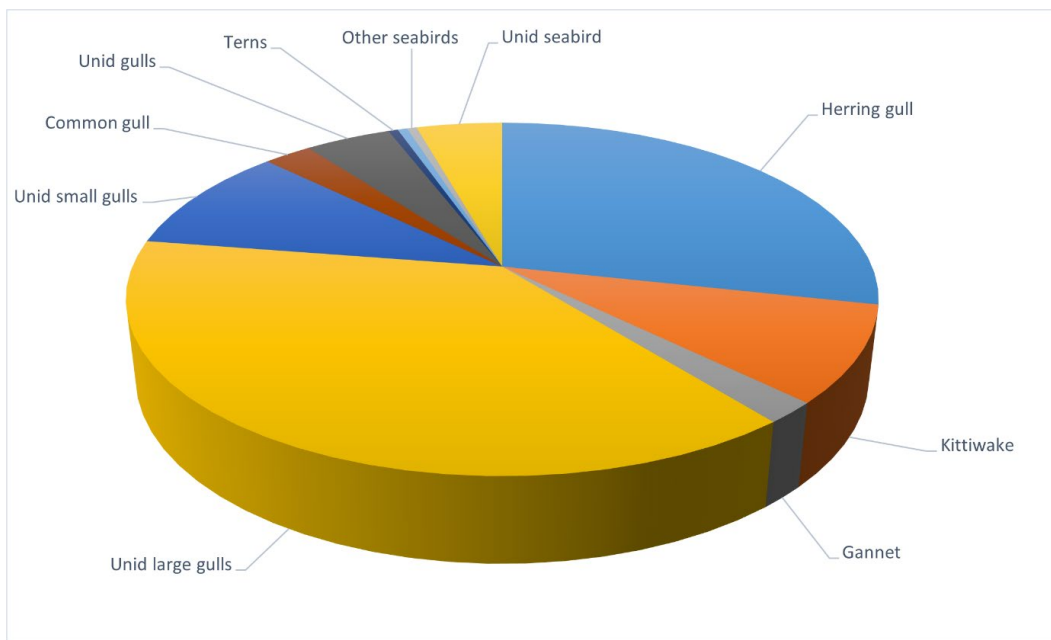Figure 14 Proportions of species and species groups in June 2020.

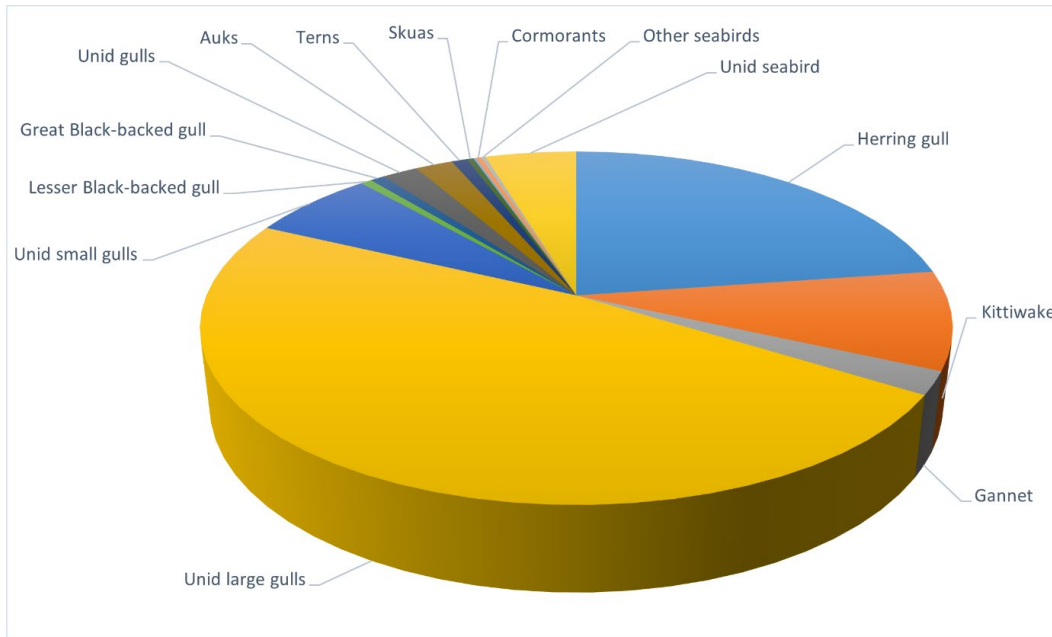Figure 15 Proportions of species and species groups in July 2020.

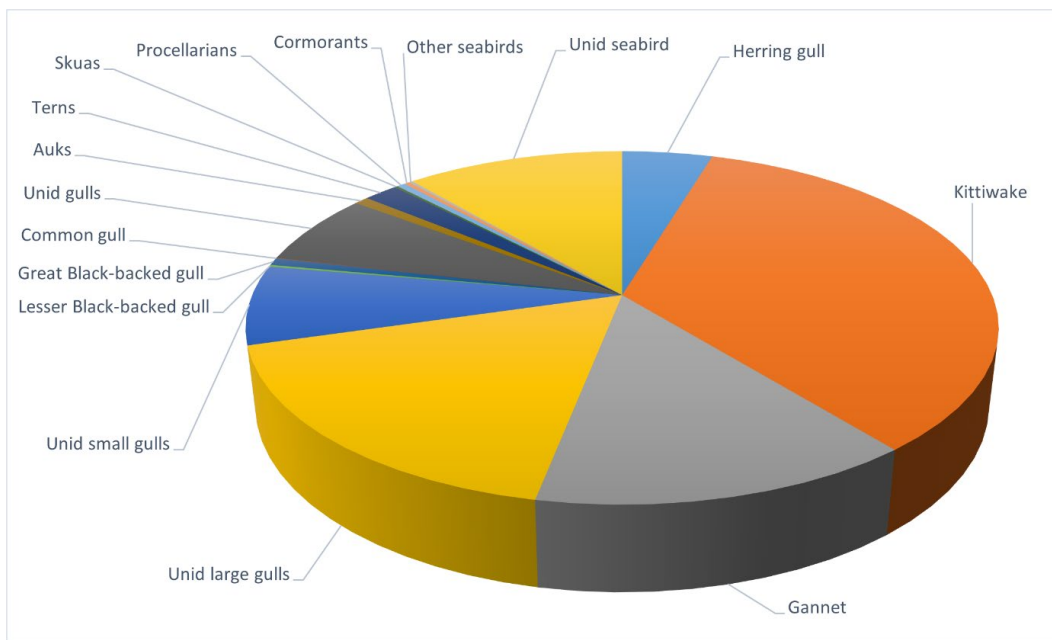Figure 16 Proportions of species and species groups in August 2020.

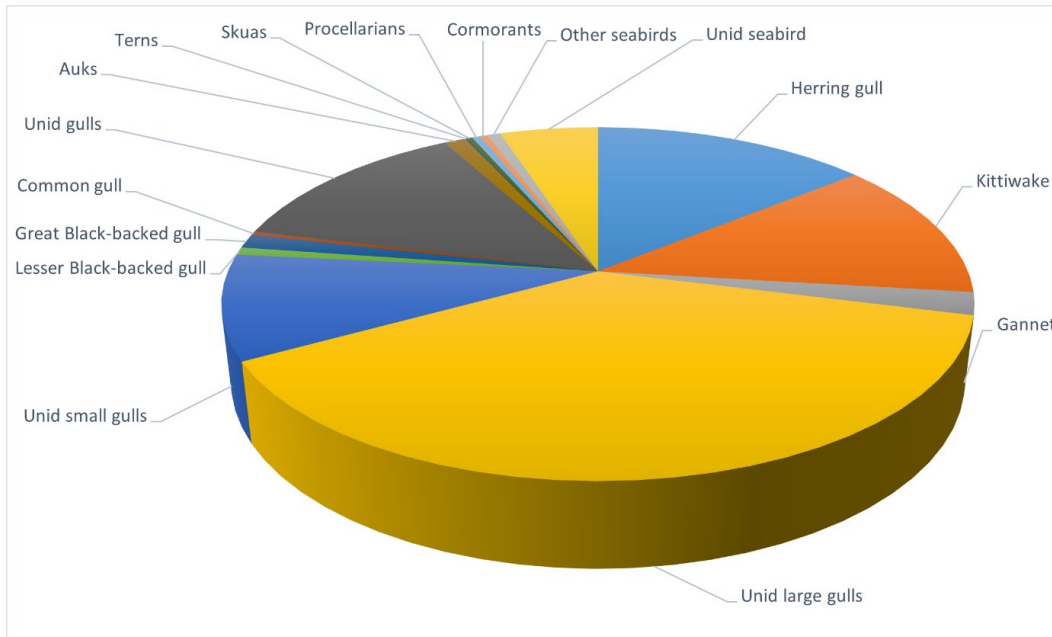Figure 17 Proportions of species and species groups in September 2020.

Figure 18 Proportions of species and species groups in October 2020.

6 Meso-avoidance

In relation to assessment of meso avoidance the cameras are mainly used to identify species tracked by the radar and to determine vertical meso avoidance taking place above/below the rotor-swept zones where the radar is blind due to shading from the turbines and blades. Target species including unidentified small and large gulls were recorded in the meso zone of the cameras in 6,318 of the bird videos (Table 4). A large proportion of the videos were unidentified gulls, yet in 33% of the large gull videos birds could be identified as herring gull and in 68% of the small gull videos birds could be identified as kittiwake. Data on vertical meso avoidance behaviour showed that in 96.8% of the video recordings the target species avoided the RSZ by flying in between the turbines with very few avoiding by changing their flight altitude in order to fly either below or above the rotors (Table 6.1). As some of the birds flying below or above the rotors apparently did not change their flight altitude on approach to the turbines the actual level of vertical meso avoidance may be even lower. This pattern of avoidance behaviour was remarkably similar for all three species of large gulls.

Overall, all gull species were both recorded moving linearly through the wind farm array with limited interactions with turbines and rotors as well as recorded feeding in between and close to turbines. Feeding in the wind farm by gulls increased markedly during August and was often associated with rafts of auks. In 23.3% of the videos target species were recorded feeding. Gulls perching on turbine transition pieces was only recorded in two videos. During linear flights target species rarely changed their direction of flight when inside the wind farm array.

Table 6.1 Meso avoidance behaviour of target species recorded by cameras between 1 April and 31 Oct 2020. Table columns "BELOW ROTOR" and "ABOVE ROTOR" indicate numbers changing their flight height in order to avoid the RSZ.

SPECIES	VIDEOS IN MESO ZONE	BELOW ROTOR	ABOVE ROTOR
Unidentified large gull	2288	13	7
Herring gull	855	14	4
Unidentified small gull	697	2	1
Kittiwake	1719	52	1
Gannet	644	16	0
Great and lesser black-backed gull	115	3	2

Patterns of track length density extracted from the radar tracks can be used to assess horizontal meso avoidance, and more specifically at which distances from turbines meso avoidance mainly takes place. An example of extracted mean track densities of gannet is displayed in Figure 19. Mean meso avoidance/attraction patterns are shown in Figure 20 displaying mean meso avoidance rates based on the formula in Skov et al. (2018) using the coupled radar track and video data calculated as $1 - \frac{N_{in}}{N_{ref}}$, where N_{in} is the mean track length per unit area within the RSZ + 10 m buffer and N_{ref} is the mean track length per unit area throughout the wind farm (inside / outside the RSZ + 10 m buffer). The meso avoidance rates have been calculated at 10 m intervals from the tip of the rotor blades to approximately half distance between turbines.

The results indicate that large gulls including herring gulls display moderate meso avoidance in the zones closer than 290 m from rotors, counterbalanced by moderate attraction to the zones in between turbines further than 290 m from rotors (Figure 20). The large gulls display the strongest avoidance behaviour (EAR 0.4/0.15) towards the turbines at distances between 80–100 m from the nearest rotor. At closer distances, unidentified large gulls and herring gulls tend to gradually reduce their avoidance response as they approach the turbines. In sharp contrast, gannets and

kittiwakes gradually increase their meso avoidance response when approaching the turbines and both species display high rates of meso avoidance (gannet 0.75, kittiwake 0.6) in close proximity to the rotors. Gannets seem to be attracted to the zones in between turbines further than 290 m from rotors, while kittiwakes are attracted to the zones further than 220 m from rotors.
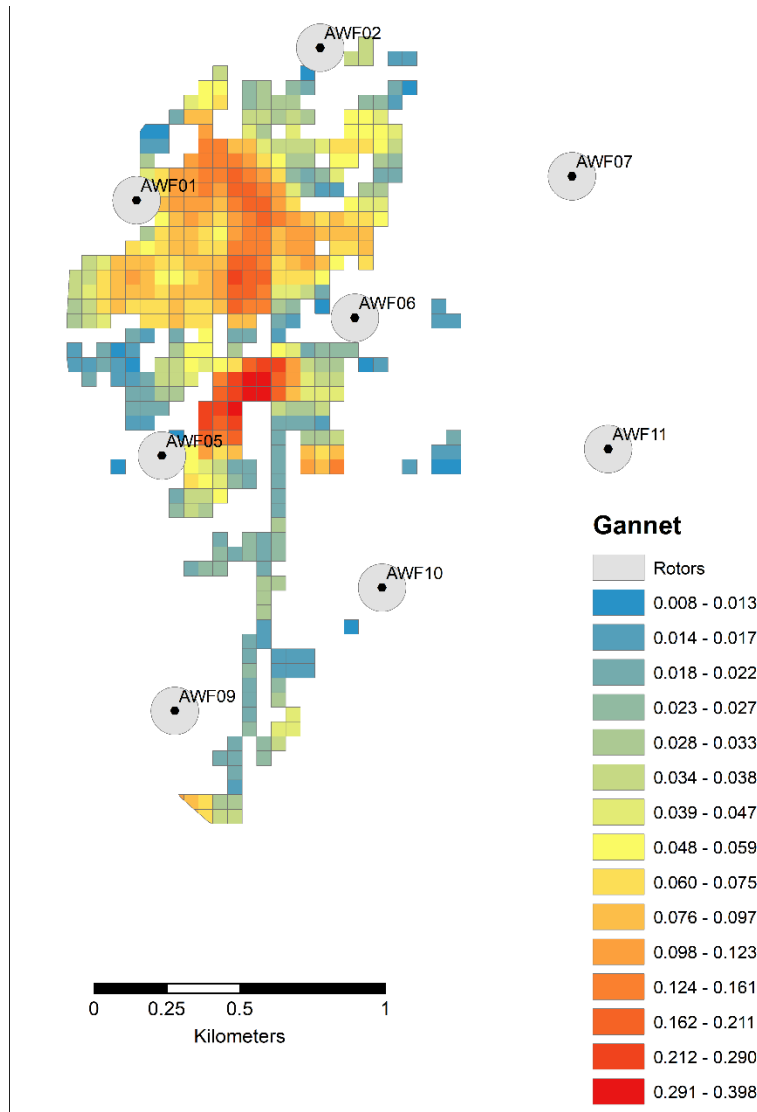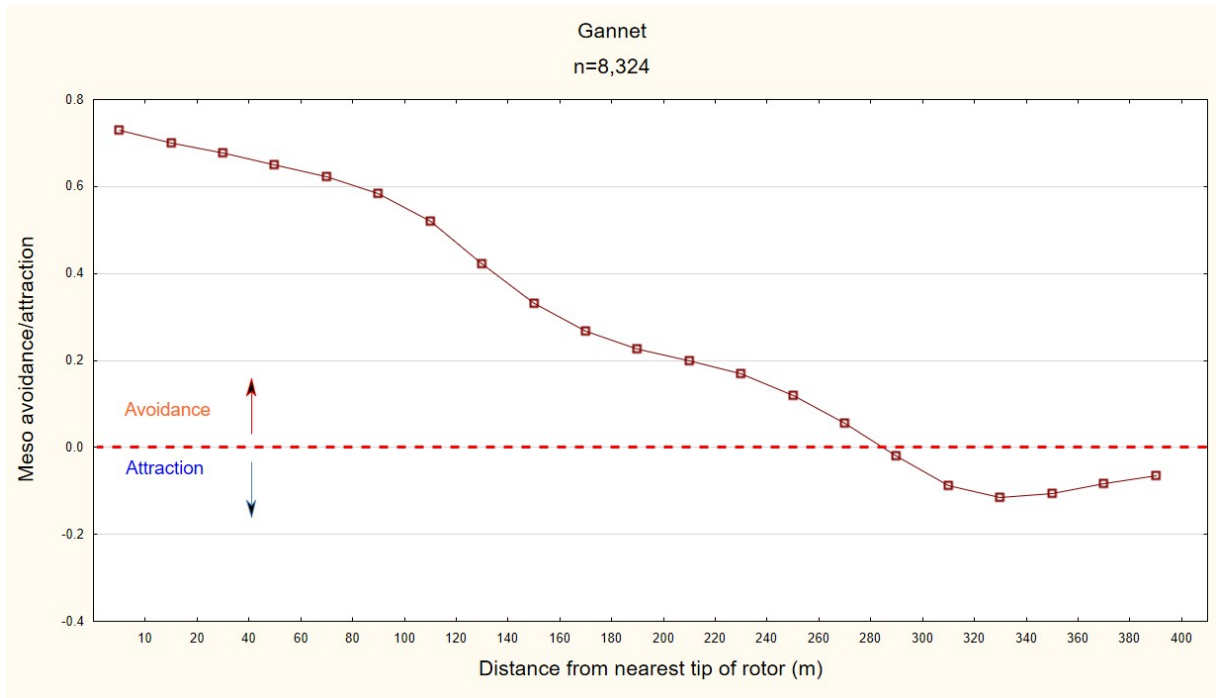

Figure 19 Mean track density of gannet recorded in the EOWDC during April-October 2020

Gannet
n=8,324

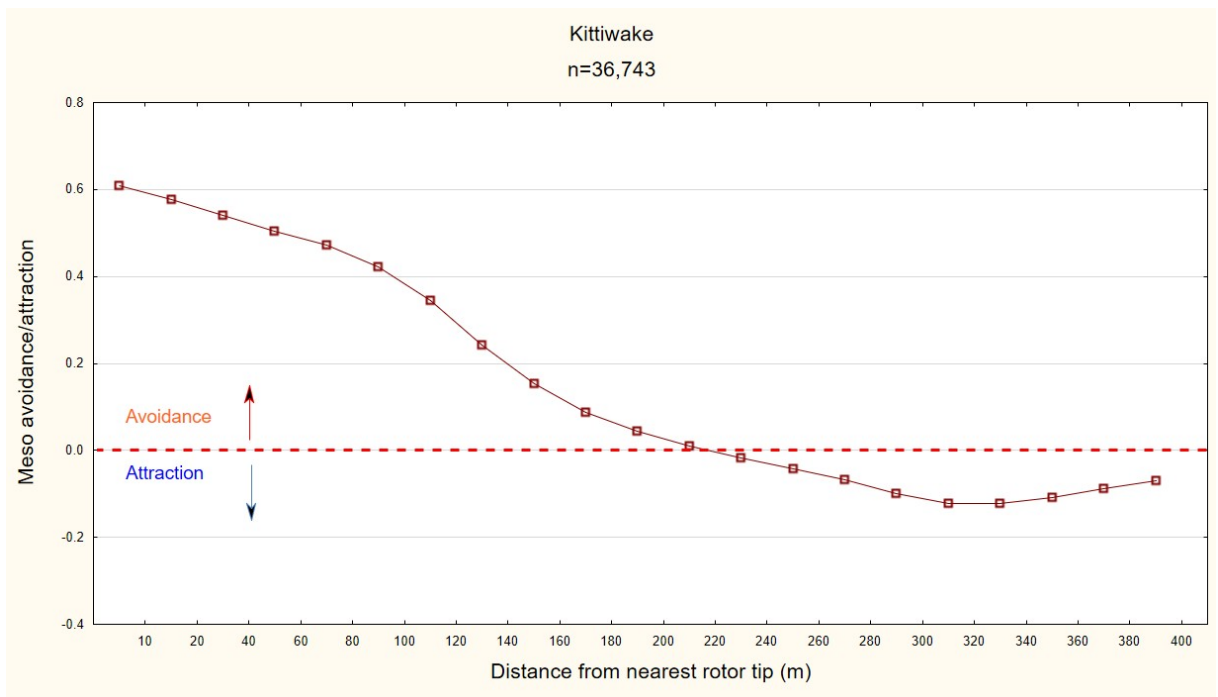Unidentified large gull
n=20,978

Figure 20 Mean meso avoidance/attraction rate of target species calculated at 10 m intervals in relation to distance from nearest rotor during daytime hours.

7   Micro-avoidance

In general, gannets, small and large gulls tended to avoid flying into the rotor swept zone defined as a circular area with a radius equivalent to the length of the rotor blades (82 m). Hence, only 196 videos with target species (3.4%) showed birds flying in the micro zone. In the vast majority of these videos target species adjusted their flight in order to avoid the spinning rotor (Table 5). The most frequently recorded adjustment of the flight was of birds flying along the plane of the rotor which was recorded in 72% of the videos of behaviour in the micro zone. In nine videos recorded in the micro zone, target species showed non-avoidance behaviour by crossing the rotor swept area without making adjustments in flight behaviour (Table 6), leading to high micro avoidance rates (Table 7).

No videos of target species showed a collision with a rotor.

Table 2 Species-specific micro avoidance behaviour of target species recorded by cameras between 1 April and 31 October 2020

SPECIES	VIDEOS IN MICRO ZONE	RETURNS	STOPS BEFORE CROSSING	ALONG ROTOR	CROSSING WITH ADJUSTMENTS
Unidentified large gulls	65	6	5	39	11
Herring gull	72	3	3	57	5
Unidentified small gull	9	1	1	5	1
Kittiwake	34	2	2	26	4
Gannet	8	1	0	7	0
Great/lesser black-backed gull	8	0	0	7	1
Total	**196**	**13**	**11**	**141**	**22**

Table 3 Species-specific micro non-avoidance behaviour of target species recorded by cameras between 1 April and 31 October 2020

SPECIES	VIDEOS IN MICRO ZONE	CROSSING WITHOUT ADJUSTMENTS	COLLISIONS
Unidentified large gulls	65	4	0
Herring gull	72	4	0
Unidentified small gull	9	1	0
Kittiwake	34	0	0
Gannet	8	0	0
Great/lesser black-backed gull	8	0	0

Mean micro avoidance rates for species or species groups with sufficient sample size are shown in Table 7 calculated as:

$$\frac{N_{birds\ adjusting\ flight}}{(N_{birds\ adjusting}+N_{birds\ not\ adjusting}+N_{birds\ colliding}}.$$

Table 4 Species-specific micro avoidance rates of unidentified large gulls, herring gulls and small gulls based on video data collected between 1 April and 31 October 2020.

| SPECIES	MEAN MICRO AVOIDANCE RATE	SAMPLE SIZE
Unidentified large gulls	0.938	65
Herring gull	0.944	72
All small gulls	0.977	43
Kittiwake	1.0	34

8   Flight altitude

The use of the combined radar track and video data for estimation of flight heights in the wind farm array was assessed by histograms (Figure 21) and by extracting the mean flight height of all target species in relation to distance from the rotors across all of the zones (Figure 22). Flight heights were obtained from combined radar tracks and camera data by triangulation of the track measurements in close to real time. Examples of 3D track trajectories are visualised in Figure 23.

The majority of gannets (58%) were recorded flying at altitudes below the lower tip height of the rotors (25 m), and all gannets were recorded flying at altitudes below the hub height. Altitudinal responses by gannets to the turbines and rotors could be identified at a distance of approximately 100 m from the rotors from which distance the flight altitude of the birds gradually declined below rotor height as they approached the RSZ. Closer to the rotors at 50 m distance for commuting birds and 25 m for feeding birds, gannets appeared to increase flight altitude and were typically recorded flying at rotor height at close proximity to the rotors.

Large gulls displayed a wide range of flight altitudes, including altitudes above the height of the rotors. However, the vast majority of both unidentified large gulls (92%) and herring gulls (87%) were recorded at altitudes below the hub height with a tendency for a concentration of flight height just below the hub. A small proportion of the large gulls were recorded flying below the rotor; unidentified gulls 11% and herring gull 18%. A change in the flight height was recorded for both commuting and feeding large gulls at a distance of approximately 125 m from the rotors and the birds increased the flight height until 45 m distance from rotors. Closer to the RSZ large gulls lowered their flight altitude to the lower part of the RSZ.

The majority of kittiwakes (56%) were recorded flying at altitudes below the rotor and all kittiwakes were recorded flying at altitudes well below the hub height. In general, there was a clear tendency for feeding kittiwakes to be recorded at slightly lower altitudes than commuting birds. A gradual decrease in the number of recorded kittiwakes was noted from 40 m height upwards to the hub height. Altitudinal responses by kittiwakes to the turbines and rotors could be identified at a distance of approximately 75 m from the rotors from which distance the flight altitude of the birds gradually declined below rotor height as they approached the rotors. Kittiwakes appeared to increase their flight height above the lower tip height of the rotors when close to the rotor, at 45 m distance for commuting birds and 25 m for feeding birds.

Gannet
n=8,324
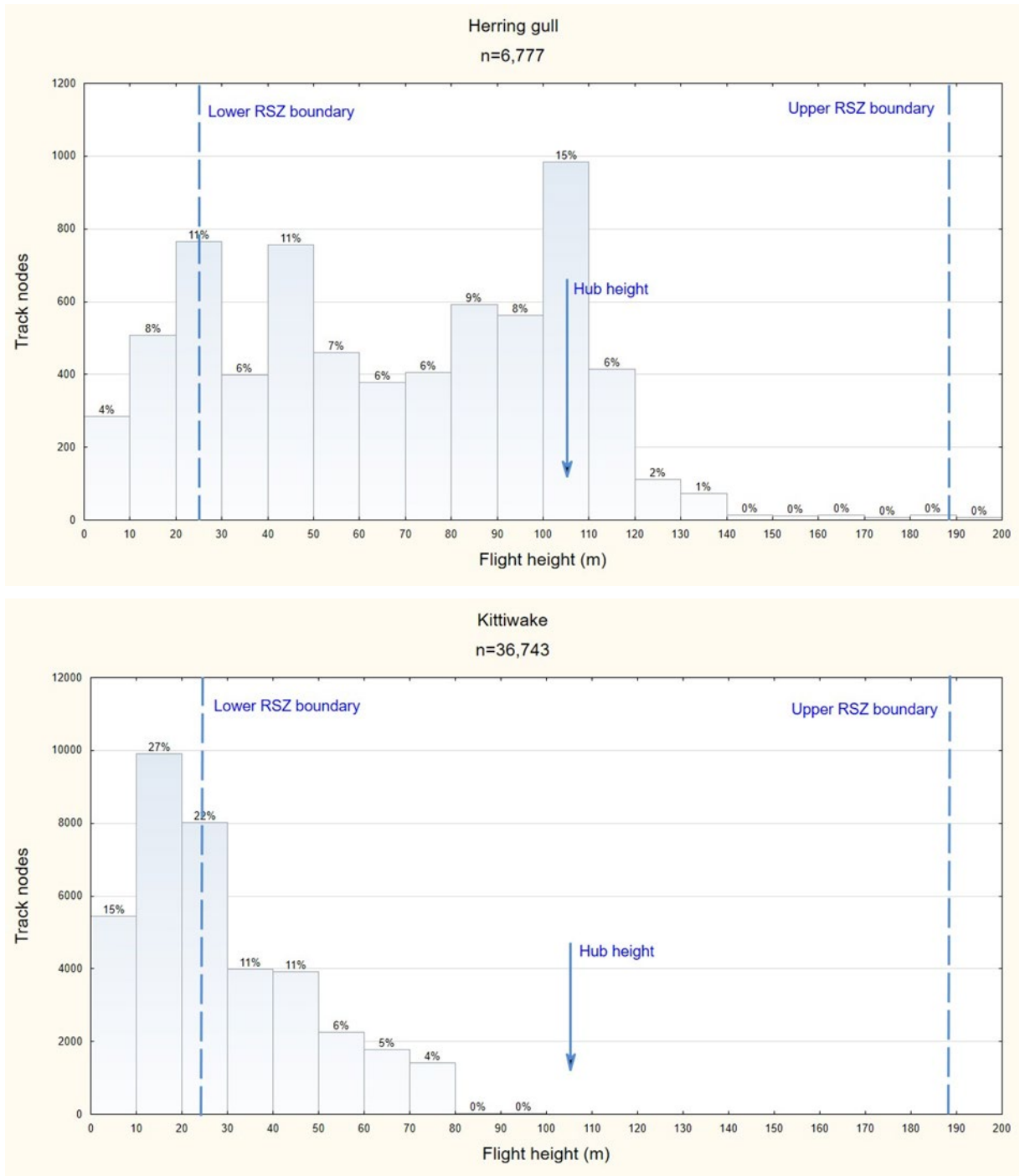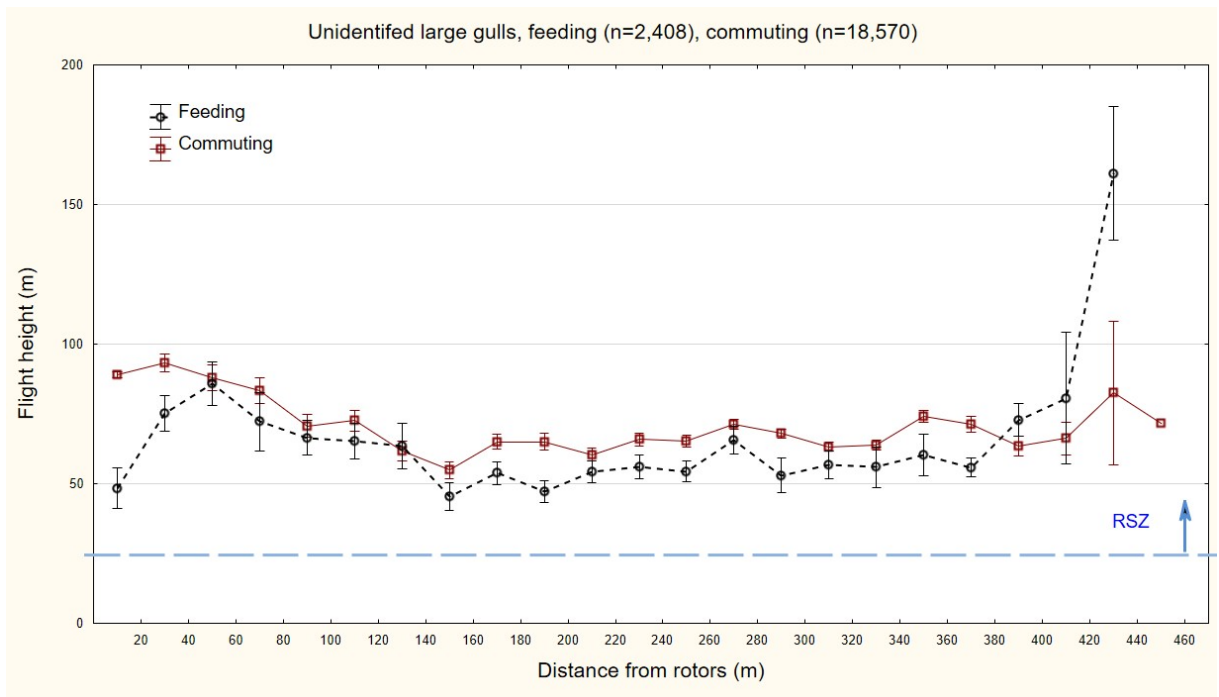

Unidentified large gulls
n=20,978
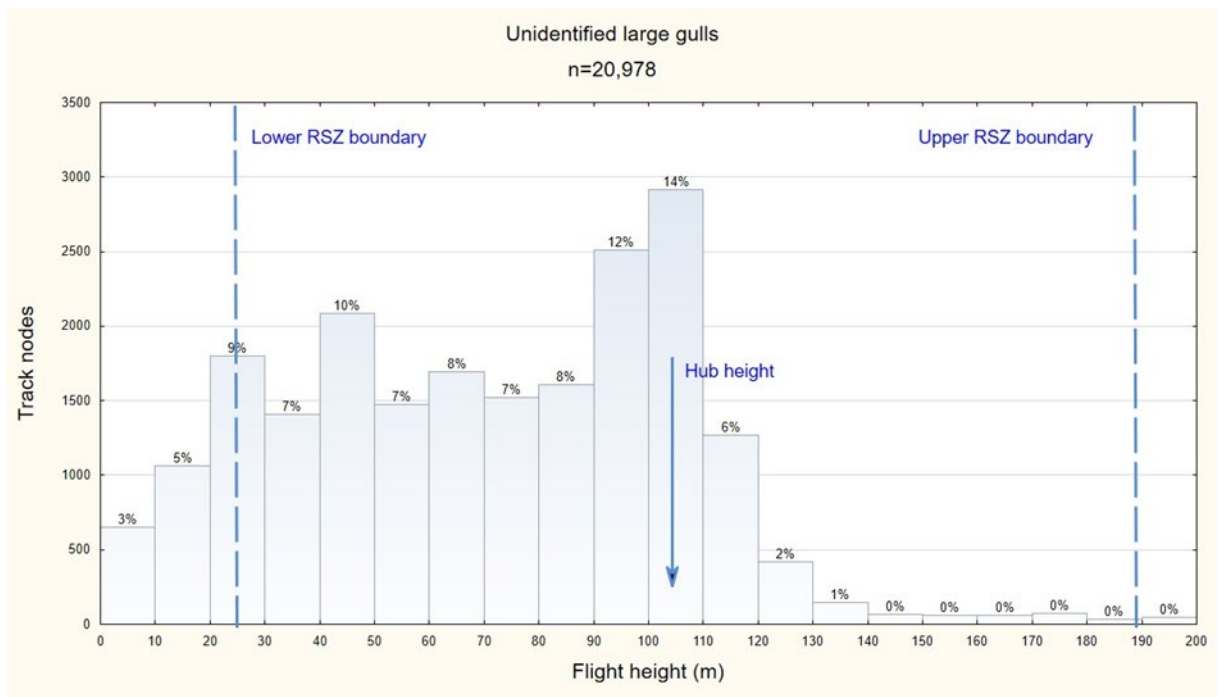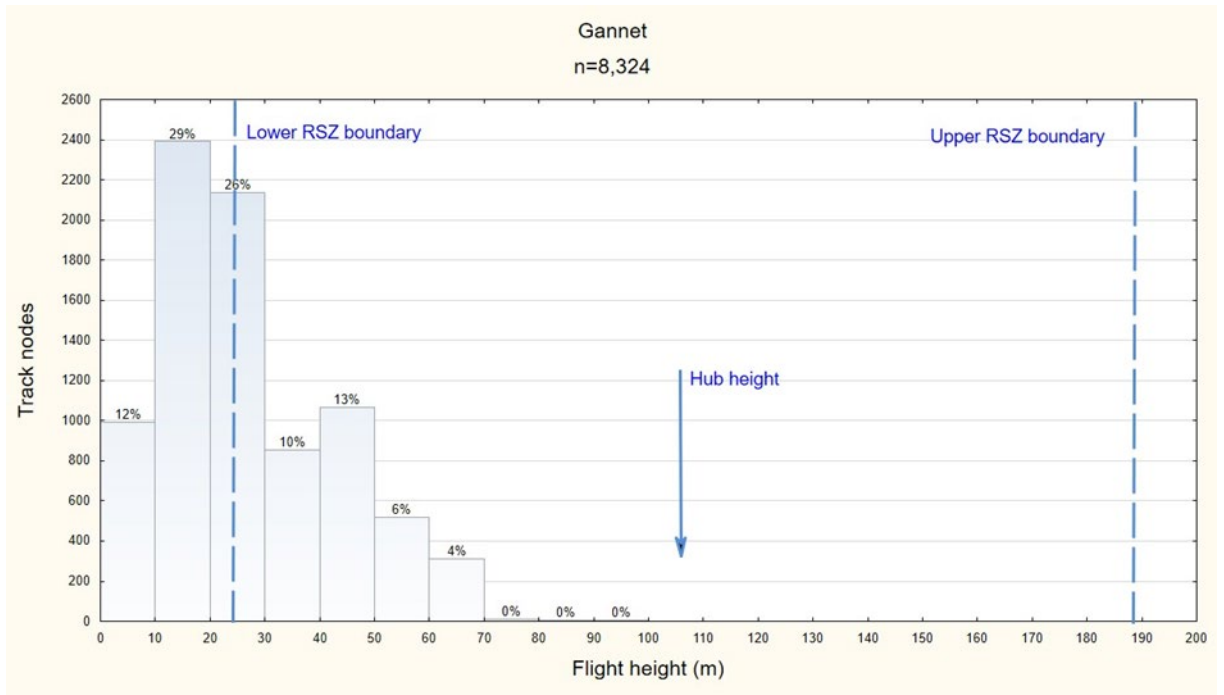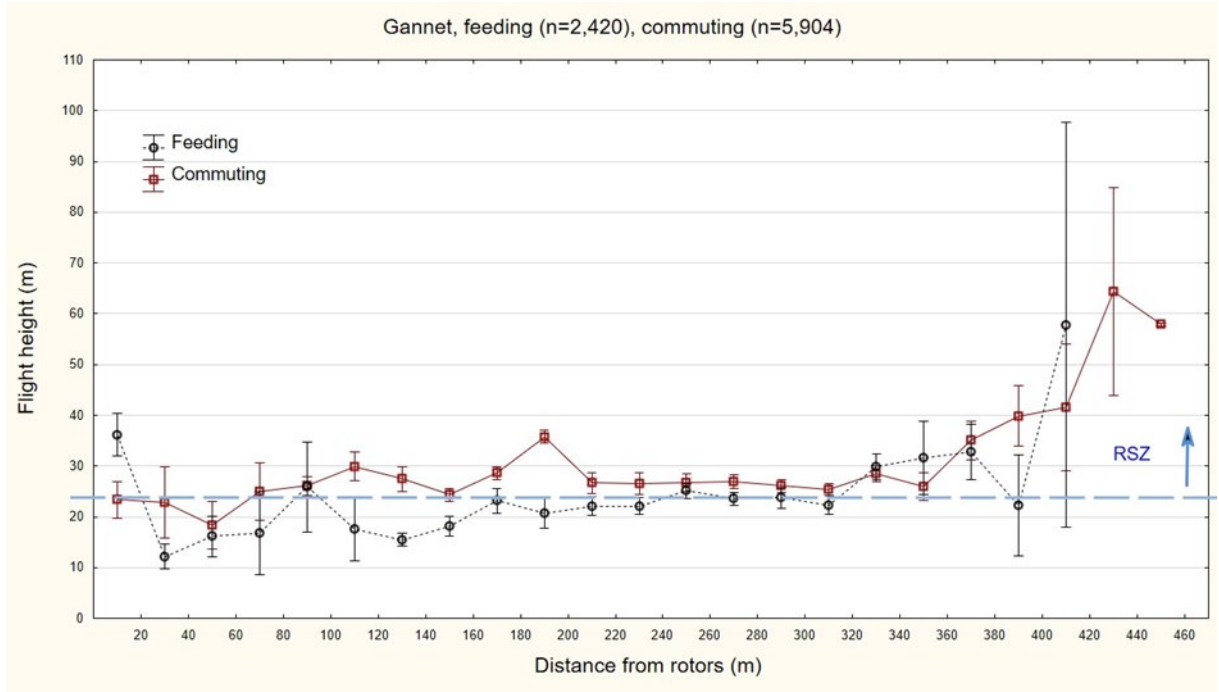
Figure 21 Histograms of flight heights of target species lower and upper boundaries of the RSZ and Hub height of turbines indicated.

Gannet, feeding (n=2,420), commuting (n=5,904)

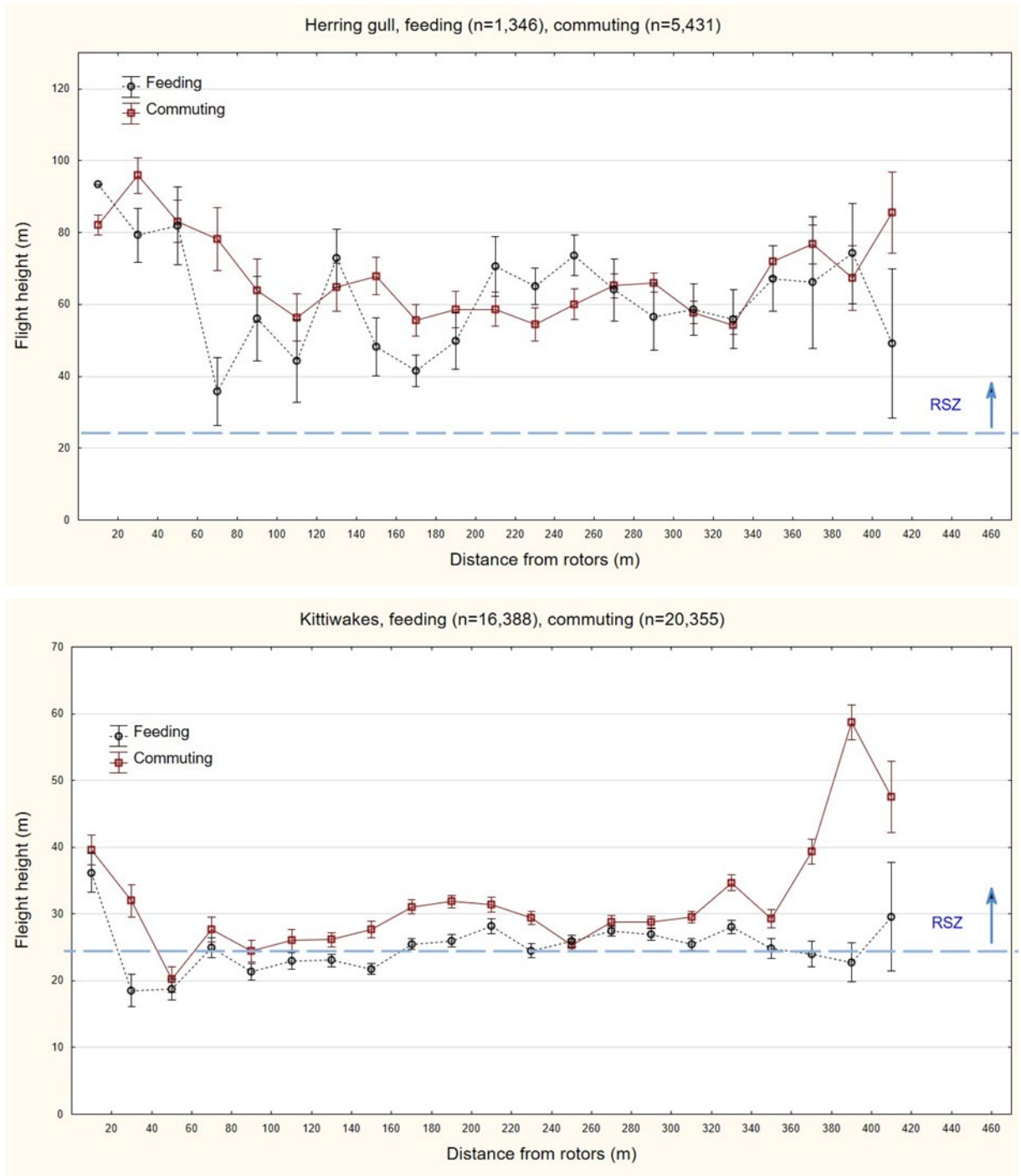Unidentifed large gulls, feeding (n=2,408), commuting (n=18,570)

Figure 22 Mean estimated flight heights of target species using triangulation and shown in relation to distance from nearest turbine during daytime hours. Lower boundary of the RSZ indicated with a blue long-dashed line.
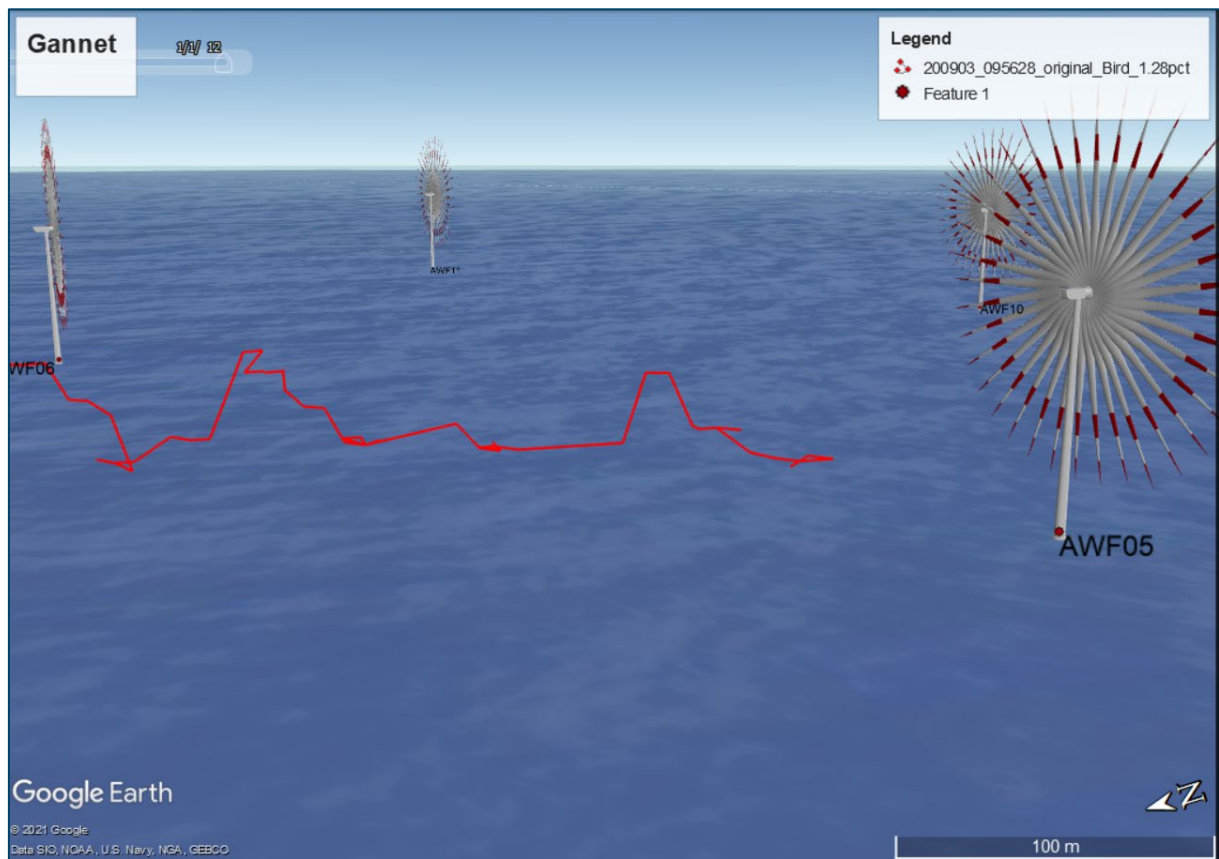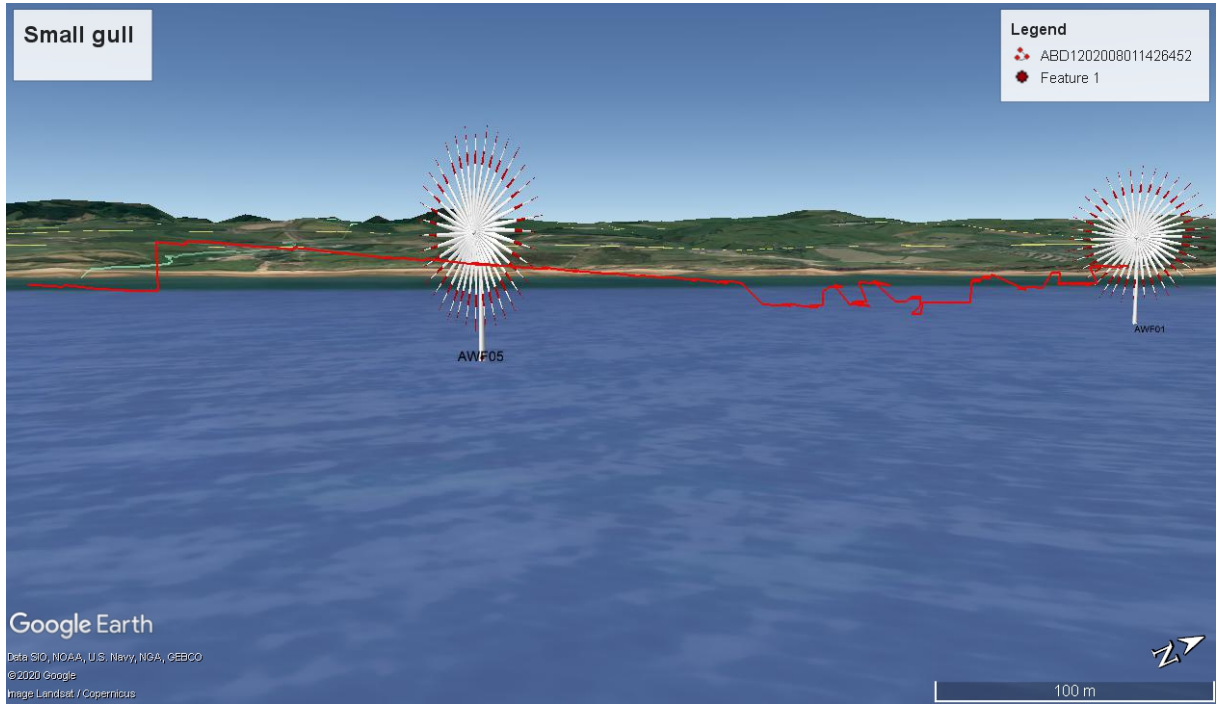
Figure 23 Examples of 3-D trajectories visualised with virtual turbines designed with correct dimensions and rotor orientation

9 Flight speeds

Combined radar track and video data also allowed for estimation of mean flight speed of the target species (Figure 24). Further than 200 m from the rotors feeding gannets were recorded flying with slightly lower speed than commuting gannets, but closer to the rotors this difference was not evident. The flight speed of gannets showed a weak tendency to decrease at distances closer than 25 m from the rotors. No clear difference in flight speeds between feeding and commuting birds were recorded for large gulls and kittiwakes. The flight speed of large gulls showed a clear tendency to decrease from 7 to 5 m/s at distances closer than 75 m (unidentified large gulls) and 65 m (herring gulls) from the rotors. The flight speed of kittiwakes decreased from 8 to 6 m/s at distances closer than 50 m from the rotors.

Gannet, feeding (n=2,420), commuting (n=5,805)
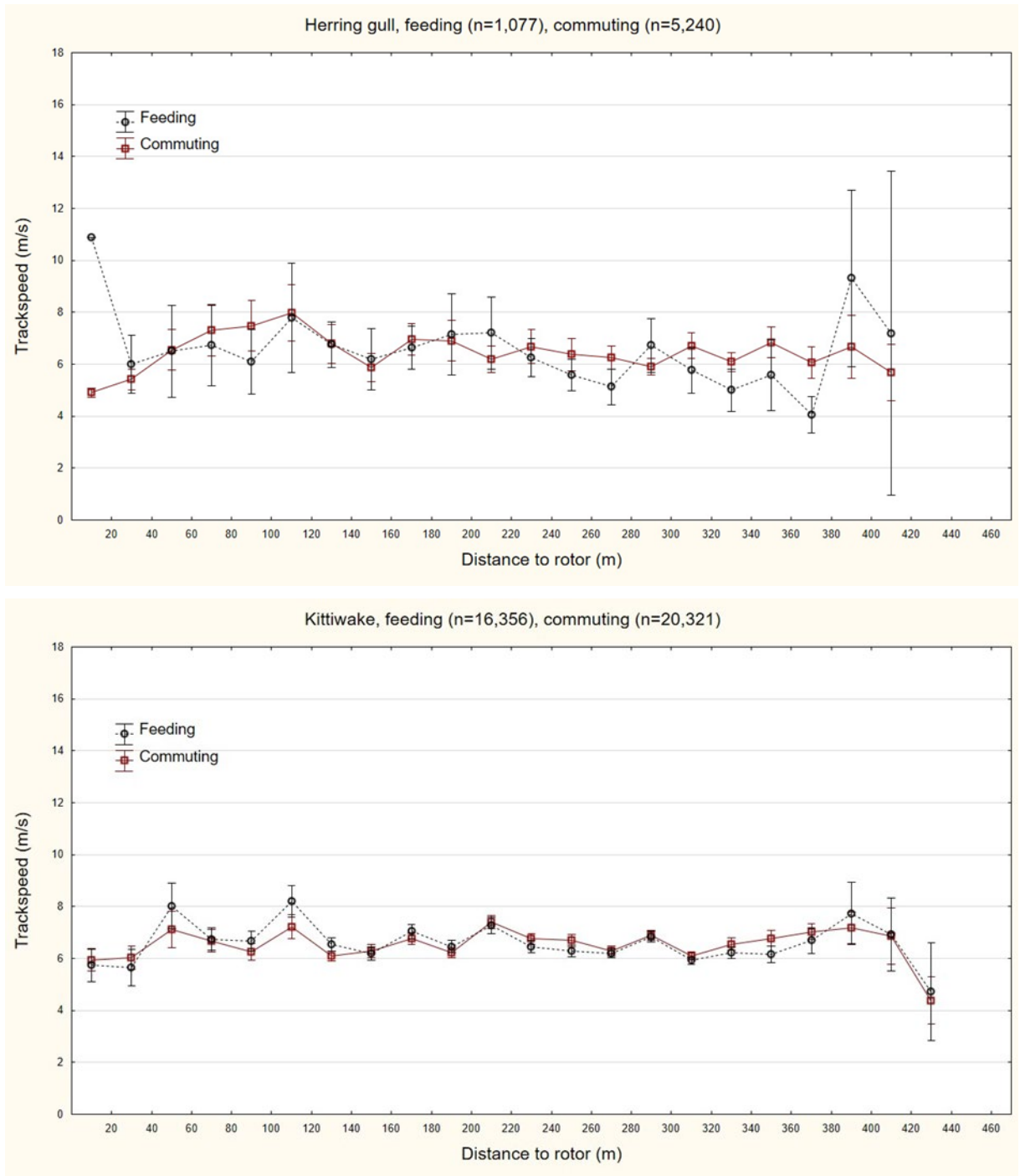

Unidentified large gulls, feeding (n=1,955), commuting (n=17,241)
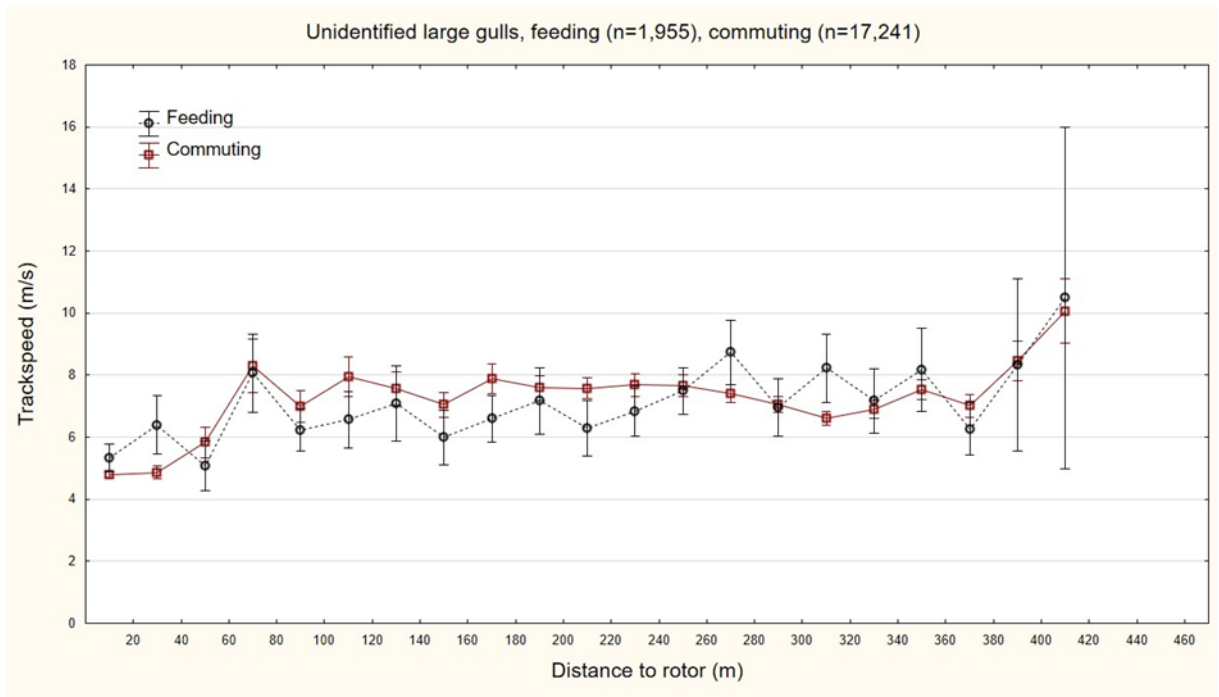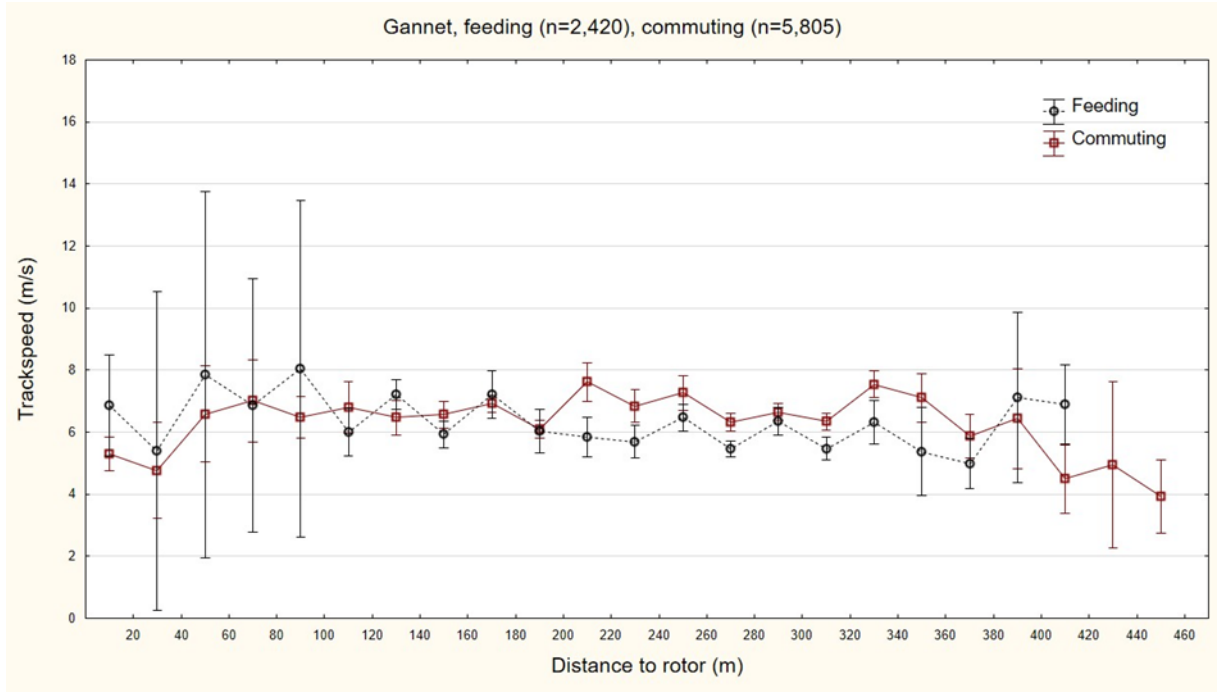
Figure 24 Mean estimated flight speed of target species in relation to distance from nearest turbine during daytime hours

10 Flight directions

Combined radar track and video data also allowed for estimation of changes in the flight direction of the target species in relation to distance from the rotors. Estimated changes in flight direction relative to the orientation of the rotor are indicated in Figure 25. Results indicated that not all target species clearly deflected when approaching a turbine. Gannets appeared to deflect around 50-100 m from the rotors, but the flight direction relative to the rotor was similar further away (>150 m) questioning whether this change of direction of flight was an actual response to the presence of the nearest rotor. Similarly, the flight response of kittiwakes in relation to distance from the turbines did not follow a clear pattern that could indicate a change in flight direction to avoid the turbines. However, a change in the direction of flight (relative to the nearest rotor) was seen among unidentified large gulls and herring gulls, which markedly deflected (7 angular degrees on average) within the closest 70 m from the nearest turbine.
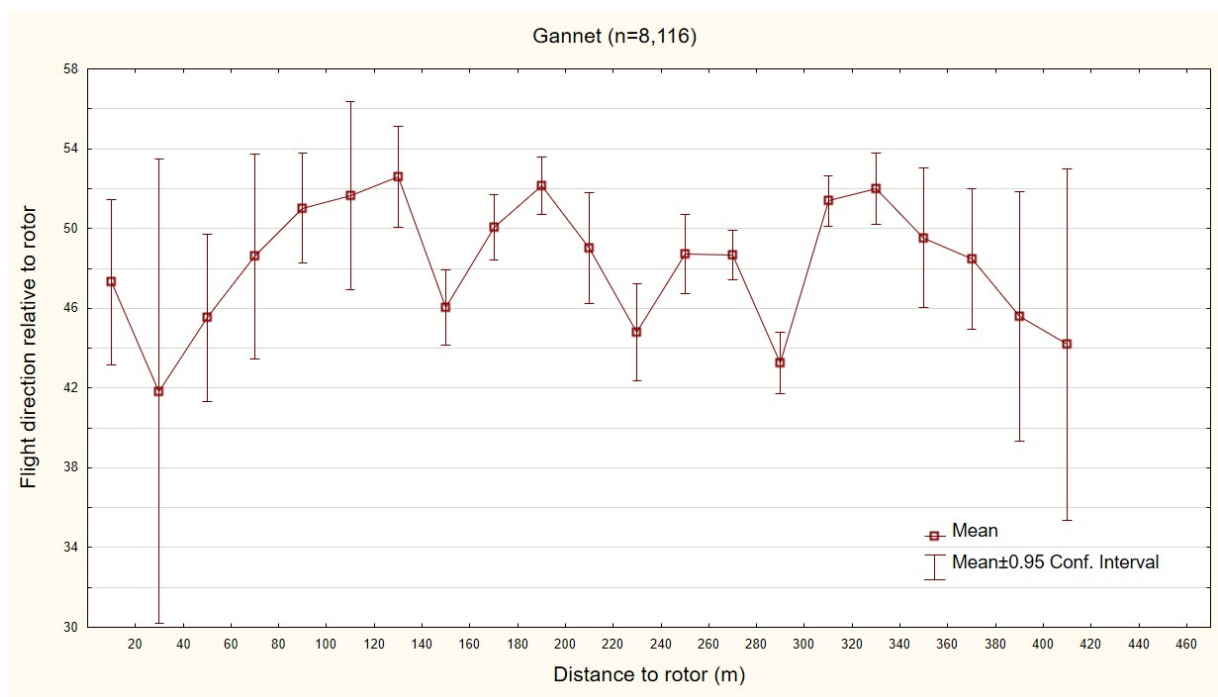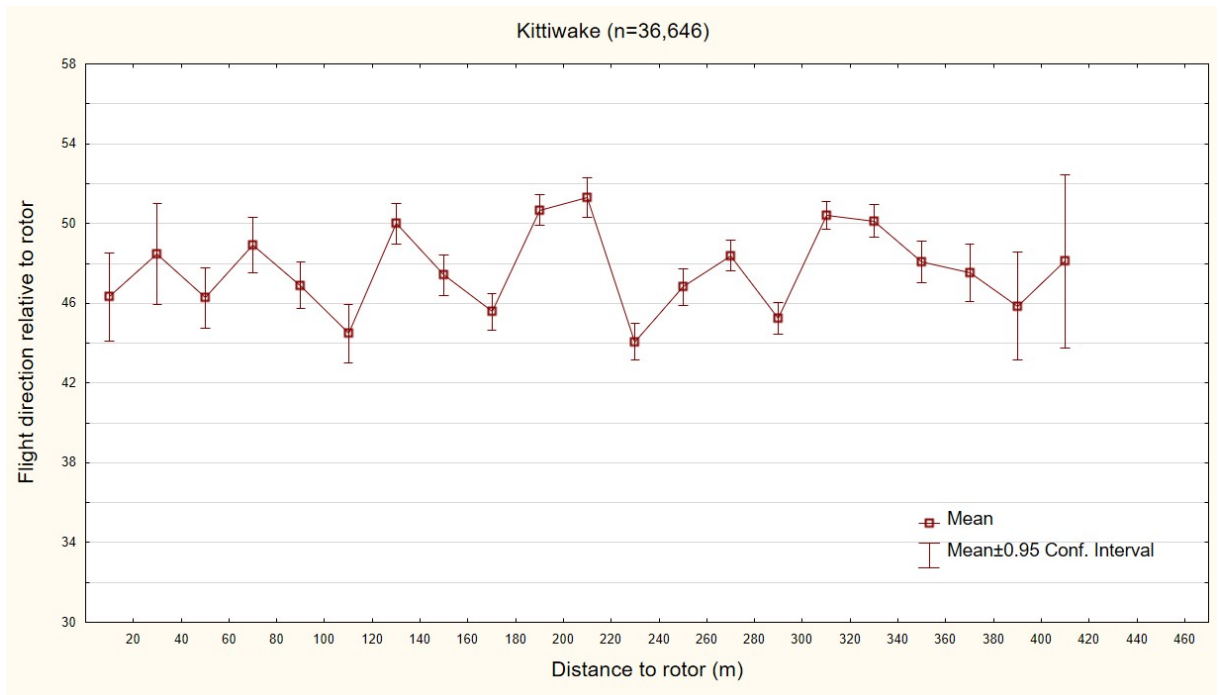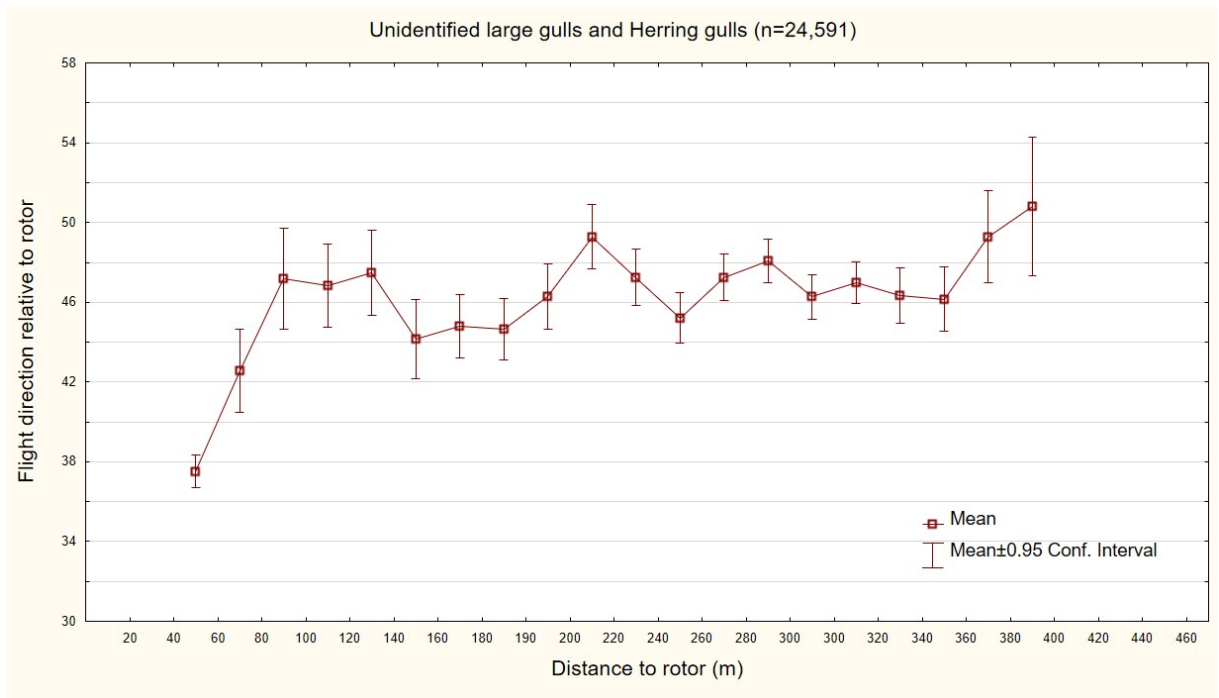
Figure 25 Mean estimated flight directions relative to the orientation of the rotor estimated for each target species in relation to distance from nearest turbine during daytime hours

11 Discussion

11.1 Sensor equipment and design

During April, May and June data collection was affected by planned power outages in the EOWDC, associated server issues and limited access to AWF6 and AWF10. After 2nd July the data collection by the detection system has been running continuously with only minor breaks and limited loss of data.

During the 2020 breeding season the equipment has been configured to operate in dual mode with the cameras' initial positions being controlled by the radar. The result is that all recorded videos have coupled radar tracks. A very large number of videos of target species were recorded during the period from mid-August to early October. Due to coupled radar and camera tracks a total of 96,000 height estimates were obtained which was beyond expectations and formed the basis for robust assessments of flight altitudes of target species in different parts of the wind farm array.

In spite of the high number of flight estimates obtained during the 2020 season the video tracker which is not based on AI (artificial intelligence) technology is suboptimal in situations with high densities of flying seabirds which occur frequently during August to October. In these situations the tracker may shift targets when there is more than one bird in the field of view, subsequently requiring manual checks and processing of the data. It has therefore been decided to upgrade the video tracker on both cameras before the 2021 season to the new version which uses deep learning algorithms to separate flying seabirds from other flying objects and has the capability to record the tracks for longer periods.

The quality of the collected video data was judged by the video analysts as acceptable. However, the RVision camera does not produce videos with the same high definition as the FLIR M400 camera. The lower resolution of the RVision videos will affect the number of videos being recorded by the new AI-tracker.

The estimated flight heights of gannets from triangulation between radar and camera data revealed results which are in line with results from tracking studies. Cleasby et al. (2015) showed a median flight height of commuting birds at 12 m and feeding birds at 27 m which fit the flight heights recorded in the EOWDC where most gannets were estimated to fly between 10 and 30 m. However, no clear difference in flight height between commuting and feeding birds was estimated in the EOWDC. The estimated flight heights of large gulls indicated that 82% of herring gulls and 89% of unidentified large gulls were flying at rotor height. Furness et al. (2013) indicate there is a large variation in defined percentage of large gull species flying at rotor height with maximum values at 90%.

The estimated flight heights for kittiwake indicated that 44% were flying at rotor height. The reported flight heights in literature is diverse and according to the review by Furness et al. (2013) varies in different studies between 0-38% at rotor height, which is slightly lower than indicated by the current study. However, the proportion of birds flying at rotor height recorded in Egmond aan Zee offshore wind farm (OWEZ) was 45% (Krijgsveld et al. 2011) and in the ORJIP study it was found to be 77% (Skov et al. 2018). At the Alpha Ventus offshore wind farm, kittiwakes were observed to prefer flight heights between 10 to 20 m (Mendel et al. 2014). Evidence from visual surveys in proposed development areas in the UK assessed flight height of 62,975 kittiwakes suggesting that 15% of flights occurred at collision risk height (Johnston et al. 2014).

The measured flight speeds from the radar track data in the wind farm are generally lower than flight speeds recorded from GPS studies outside wind farms. These studies are generally, however, large scaled and therefore also include "transition flights" from colonies to feeding grounds, long sustained directional flights. Pettex et al. (2012) reported a mean flight speed of about 13.5 m/s for gannet in comparison to the 6-8 m/s measured in this study. Flight speed of lesser black-backed gulls based on GPS measurements (Gyimesi et al. 2016) from two different studies was 12.5 m/s and 10.7 m/s as compared to 5-8 m/s measured for herring gulls and

unidentified large gulls in this study. GPS flight speed for kittiwake was reported by Kotzerka et al. (2010) and Elliot et al. (2014) to be 9.2 m/s and 10.6 m/s respectively as compared to 6.5-7.0 m/s measured in this study. Flight speed is an important parameter in the Band collision risk model; for example a change in flight speed of gannet from 13.5 m/s to 8 m/s could reduce the risk estimated by the model by more than 20%.

In order to improve the probability to record flight data in adverse weather conditions it was decided to install two weather stations at AWF6 and AWF10. These were installed in February 2021. The two weather stations will facilitate control of the operating modes during different wind conditions. The two weather stations (Young Ultrasonic Anemometer) are now installed on turbine AWF10 and will control the shift between dual and solo sensor mode. Wind speed measurements are integrated with the MUSE software in real-time, and when the wind speed exceeds a predefined threshold, the mode is switched to solo mode. Based on the data collected during 2020 the need to operate the cameras in solo mode during wind conditions below the predefined threshold will be assessed. For the 2021 season the digital communication between radar and cameras has been configured so that the cameras are turned into solo mode during wind speeds > 15 m/s.

11.2   Analytical framework

The species identification for both meso and micro avoidance requires analyses of the collected video data. The four target species herring gull, lesser and great black-backed gull and kittiwake are particularly difficult to separate in the field, and even more so on video where characteristics like size, motion features and jizz (general impression and shape) look different from when viewed in the field. In order to validate the species identifications, all gull videos were checked by an independent observer.

Although the radar tracks used for the estimation of meso avoidance are selected from the pool of all radar tracks, the selection is based on first detection and therefore as close to random as possible. As the calculation of the meso avoidance rates is based on proportional statistics the results for meso avoidance are judged as unbiased even if it is based on a subset of all tracks. The same holds true even if a lower proportion of the birds are recorded by the radar during high sea states (> Beaufort 4) due to the use of dynamic clutter filtering. Based on the power assessments for the ORJIP project the target sample size per species for meso avoidance estimation is 250. Given the available sample from the first year of monitoring it seems clear that this target has already been met for gannet, herring gull and kittiwake. As determined from the recorded patterns of track length density all three species and unidentified large gulls displayed horizontal meso avoidance within 100 m distance from the rotors, and as expected they also displayed attraction to the areas in between the turbine rows. Large gulls including herring gulls showed moderate meso avoidance (unidentified large gulls 0.4 and herring gull 0.15) peaking at distances between 80–100 m from the nearest rotor, whereas gannets and kittiwakes gradually increased meso avoidance response from 100 m to 0 m and displayed high rates of meso avoidance (gannet 0.75, kittiwake 0.6) in close proximity to the rotors.

At distances within 100 m from the rotors the recorded meso avoidance response behaviour for all three species and unidentified large gulls seemed to be manifested as a complex 3-dimensional pattern. The meso avoidance analyses indicated that the initial response by gannets was to reduce the flight altitude below the lower tip height of the rotor, followed by an increase in flight height and a decrease in flight speed in close proximity to the rotors. The data indicate that this altitudinal response took place closer to the rotors (25 m) for feeding than commuting gannets. The fact that gannets did not display a change in the flight direction relative to the rotors as they approached the turbines and very few birds (8) were recorded in the RSZ corroborate the finding of a very high meso avoidance rate (0.75) of the species in the EOWDC. In comparison in the ORJIP project a meso avoidance rate of 0.921 (± 0.174 SD) was estimated for gannet (Skov et al. 2018). As the distances of birds to rotor-swept zones in the ORJIP project was determined based on the video

documentation, and track lengths were estimated based on mean track speeds the meso avoidance rates from the EOWDC project are the first rates which have been based on a combination of detailed radar and camera tracks and are therefore likely to be more reliable. As the radar and camera track data allow resolving densities at 15-20 m spatial resolution with an uncertainty of less than 20% these fine-scale patterns are judged as robust. Data collection during the second year of the study will reveal whether the patterns persist.

The only other empirical study which has reported on meso avoidance is the monitoring study in the OWEZ OWF in the Netherlands where Krijgsveld et al. (2011) reported a meso avoidance rate of 0.66 for all species combined. Cook et al. (2018) reviewed existing evidence from monitoring programs and suggested that meso avoidance rates may vary between sites. The data from EOWDC indicate that commuting gannets show a slightly stronger meso avoidance response than feeding gannets as reflected by differences in vertical meso avoidance pattern between the two groups.

The behavioural responses by large gulls closer to the rotors as reflected by herring gulls and unidentified large gulls showed a decrease in flight speed at 65-75 m and a decrease in flight height at 45 m followed by a change in flight direction on approach (decreasing angle) to the rotors. Accordingly, in close proximity to the RSZ large gulls increased flight height and frequently made horizontal adjustments to their flight path to fly along the plane of the rotor as corroborated by the video analyses of micro avoidance behaviour. These patterns were identical between commuting and feeding birds. The result of this flight behaviour is a lower level of meso avoidance as compared to the gannet, yet a strong micro avoidance (unidentified large gulls 0.938 and herring gull 0.944). A similar micro avoidance rate (0.957 ± 0.115 SD) was estimated for large gulls in the ORJIP project using the same methods as in this project (Skov et al. 2018).

Kittiwakes seemed to respond to the rotors in a similar way to gannets by initially reducing the flight altitude below the lower tip height of the rotor, followed by an increase in flight height and a decrease in flight speed in close proximity to the rotors. Like for gannets the altitudinal response took place closer to the rotors (25 m) for feeding than commuting birds. However, although kittiwakes did not display a change in the flight direction relative to the rotors as they approached the turbines some birds were recorded in the RSZ where the video analyses showed a micro avoidance behaviour of the birds by flying along the plane of the rotor. Hence, the avoidance behaviour of kittiwake could be seen as intermediate between that of gannet and large gulls with moderate to high level of meso avoidance and a very high level of micro avoidance.

In future, it is intended to extend the analysis in two key areas. First, by examining differences in bird flight behaviours between feeding and commuting birds. In the 2020 season, the behaviour of the birds in flight was classified subjectively by the video analysts as feeding or commuting based on the definitions of behaviour in ESAS codes. For the 2021 season, the determination of feeding and commuting birds will be based on assessments of both video and radar track data to improve the objectivity in defining the behaviour of the birds observed. Second, further analysis will be undertaken to investigate the influence of weather conditions on bird flight behaviour, such as the relationship between wind speed and wind direction of the birds' flight heights and flight speeds.

The target sample size for calculation of species-specific micro avoidance rates is 100 (Skov et al. 2018). Given the available sample in the micro zone from the first year of monitoring it seems that this target most likely will be difficult to meet for gannet. The consequence of the recorded avoidance responses of the target species within the EOWDC wind farm is that gannet shows the strongest overall avoidance, while large gulls show the slightly weaker overall avoidance with kittiwake being intermediate between the two. The avoidance behaviour of gannet was mainly exhibited at the meso level, of large gulls mainly at the micro level and of kittiwakes at both meso and micro levels. The resulting combined overall within wind farm avoidance is deemed to be very high for all target species and at least at the level documented in the ORJIP project. This is also mirrored by the absence of any observed collisions in the more than 6,000 analysed videos despite the high densities of the target species during August-October.

12 References

Cook, A.S.C.P, Humphreys, E.M., Bennet, F., Masden, E.A., Burton, N.H.K. 2018 Quantifying avian avoidance of offshore wind turbines: Current evidence and key knowledge gaps. Mar Environ Res. 140: 278-288. doi: 10.1016/j.marenvres.2018.06.017.

Cleasby, I.R., Wakefield, D.E., Bearhop, S., Bodey, T.W., Votier, S.C. and Hamer, K.C. 2015. Three-dimensional tracking of a wide-ranging marine predator: flight heights and vulnerability to offshore wind farms. Journal of Applied Ecology 52: 1-9.

Elliot, K.H., Chivers, L., Bessey, L., Gaston, A.J., Hatch, S.A., Kato, A., Osborne, O., Ropert-Coudert, Y., Speakman, J.R. and Hare, J.F. 2014. Windscapes shape seabird instantaneous energy costs but adult behaviour buffers impacts on offspring. Movement Ecology 2014, 2: 1-15.

Furness, R., Wade, H. and Masden, E. 2013. Assessing vulnerability of marine bird populations to offshore wind farms. Journal of Environmental Management 119: 56–66.

Gyimesi, A., Boudewijn, T.J., Buijs, R.J., Shamoun-Baranes, J.Z. and others. 2016. Lesser black-backed gulls Larus fuscus thriving on a non-marine diet. Bird Study 63: 241-249.

Johnston, A., Cook, A.S.C.P., Wright, L.J., Humphreys, E.M. and Burton, N.H.K. 2014. Modelling flight heights of marine birds to more accurately assess collision risk with offshore wind turbines. Journal of Applied Ecology 51: 31-41.

Kotzerka, J., Garthe, S. and Hatch, S.A. 2010. GPS tracking device reveal foraging strategies of Black-legged Kittiwakes. Journal of Ornithology 151: 459-467.

Krijgsveld, K.L., Fijn, R., Japink, M., Van Horssen, P., Heunks, C., Collier, M., Poot, M.J.M., Beuker, D., Dirksen, S. 2011. Effect studies offshore wind farm Egmond aan Zee. Final Report on fluxes, flight altitudes and behaviour of flying birds. Bureau Waardenburg bv. Nordzee Wind. 330pp.

Mendel, B., Kotzerka, J., Sommerfeld, J., Schwemmer, H., Sonntag, N. and Garthe, S. 2014. Effects of the Alpha Ventus offshore test site on distribution patterns, behaviour and flight heights of seabirds. In: Federal Ministry for the Environment, Nature Conservation and Nuclear Safety (Eds.) Ecological Research at the Offshore Windfarm alpha ventus, pp95 – 110. DOI: 10.1007/978-3-658-02462-8_11.

Pettex, E., Lorentsen, S.H., Gremillet, D., Gimenez, O., Barrett, R.T., Pons, J.B., Le Bohec, C. and Bonadonna, F. 2012. Multi-scale foraging variability in Northern Gannet (Morus bassanus) fuels potential foraging plasticity. Marine Biology 159: 2743-2756.

Skov, H., Heinänen, S., Norman, T., Ward, R.M., Méndez-Roldán, S. & Ellis, I. 2018. ORJIP Bird Collision and Avoidance Study. Final report – April 2018. The Carbon Trust. United Kingdom. 247 pp.